Low Field Magnetic Response of the Granular Superconductor $La_{1.8}Sr_{0.2}CuO_4$

L. Leylekian, M. Ocio and L. A. Gurevich *
Service de Physique de l'Etat Condensé, CEA,
CE Saclay, 91191 Gif sur Yvette Cedex

M. V. Feigel'man
Landau Institute for Theoretical Physics, Moscow, 117940, Russia.

February 1, 2008

Abstract

The properties of the low excitation field magnetic response of the granular high temperature (HT_c) superconductor $La_{1.8}Sr_{0.2}CuO_4$ have been analyzed at low temperatures. The response of the Josephson currents has been extracted from the data. It is shown that intergrain current response is fully irreversible, producing shielding response, but do not carry Meissner magnetization. Analysis of the data shows that the system of Josephson currents freezes into a glassy state even in the absense of external magnetic field, which is argued to be a consequence of the d-wave nature of superconductivity in $La_{1.8}Sr_{0.2}CuO_4$. The macroscopic diamagnetic response to very weak variations of the magnetic field is shown to be strongly irreversible but still qualitatively different from any previously known kind of the critical-state behaviour in superconductors. A phenomenological description of these data is given in terms of a newly proposed "fractal" model of irreversibility in superconductors.

PACS numbers 74.50.+r, 74.60.Ge, 74.80.Bj

*Permanent address: Institute of Solid State Physics, Chernogolovka, Moscow Region, 142432, Russia. Current address: Delft University of Technology, Lorentzweg 1, 2628 CJ Delft, The Netherlands.

I Introduction

Granular superconductors (SC) are composed of a very large number of small (micron-size) superconductive grains which are coupled together due to the Josephson tunnelling (or, in some cases, due to the proximity effect). These systems are inherently disordered due to randomness in the sizes of grains and in their mutual distances. Usually the strength of Josephson coupling between grains is rather weak, so the maximum Josephson energy of the contact between two grains is much below the intragrain superconductive condensation energy. Therefore granular SC can be considered as systems with a two-level organization: their short-scale properties are determined by the superconductivity of individual grains, whereas the macroscopic SC behaviour is governed by the weak intergrain couplings. In the treatment of the latter, one can neglect any internal structure of SC grains and describe them just by the phases ϕ_j of their superconductive order parameters $\Delta_j = |\Delta|_j \exp(i\phi_j)$. As a result, the macroscopic behaviour of granular SC can be described by a classical free energy functional of the form (cf. Ref. [1, 2, 3]):

$$H = \frac{1}{2}\sum_{ij} E_J^{ij} cos(\phi_i - \phi_j - \alpha_{ij}) + \int d^3r \left(\frac{1}{8\pi}(rot\mathbf{A})^2 - \frac{1}{4\pi} rot\mathbf{A}\cdot\mathbf{H}_{ext} \right) \qquad \text{(I.1)}$$

where $\alpha_{ij} = \frac{2\pi}{\Phi_0}\int_i^j \mathbf{A}d\mathbf{r}$ is the phase difference induced by the electromagnetic vector potential $\mathbf{A}$ and $\Phi_0 = \pi\hbar c/e$, whereas the coupling strengths E_J^{ij} are proportional to the maximum Josephson currents: $E_J^{ij} = \frac{\hbar}{2e} I_{ij}^c$. The vector potential $\mathbf{A}$ in Eq.(I.1) is the sum of the vector potential $\mathbf{A}_{ext}$ of the external magnetic field $\mathbf{H}_{ext}$ and of the Josephson currents-induced vector potential $\mathbf{A}_{ind}$. In the absence of external magnetic field, the lowest-energy state for the "Hamiltonian" (I.1) is, clearly, a macroscopically superconductive state with all phases ϕ_j equal to each other. Thus that granular SC system looks similar to the random XY ferromagnet with randomness in the values of the coupling strengths E_J^{ij}'s (apart from the possible role of the induced vector potential $\mathbf{A}_{ind}$ which will be dicussed later); within this analogy the role of XY "spin components" is taken by $S_x = \cos\phi_j$, $S_y = \sin\phi_j$.

The situation becomes a lot more complicated in the presence of non-zero external magnetic field $\mathbf{H}_{ext}$, which makes the system *randomly frustrated* (since magnetic fluxes penetrating plaquettes between neighbouring grains are random fractional parts of Φ_0). When the external field is sufficiently strong, $H_{ext} \gg H_0 = \Phi_0/a_0^2$ (here a_0 is the characteristic intergrain distance), the random phases α_{ij} become of the order of π or larger, which means complete frustration of the intergrain couplings – i.e. the system is then expected to resemble the XY *spin glass*. Actually the random Josephson network in a magnetic field is not exactly identical to the XY spin glass due to the following reasons [1]: i). The effective couplings $\tilde{E}_J^{ij} = E_J^{ij}\exp(i\alpha_{ij})$ between "spins" $\mathbf{S_i}$ of the frustrated SC network are *random complex* numbers whereas in the XY spin glass model, they are *real random* numbers. ii). Generally the phases α_{ij} depend on the total magnetic induction $\mathbf{B} = \mathbf{H}_{ext} + \mathbf{B}_{ind}$, i.e. the effective couplings $\tilde{E}_J^{ij}$ depend on the phase variables ϕ_j determining the intergrain currents $I_{ij} = I_{ij}^c sin(\phi_i - \phi_j - \alpha_{ij})$. In some cases the effects produced by the self-induced magnetic field $\mathbf{B}_{ind}$ are weak and can be neglected (the quantitative criterion will be discussed later on), so that phases α_{ij} can be considered as being fixed by the external field.

The model described by the Hamiltonian (I.1) with fixed α_{ij}'s and $H_{ext} \gg H_0$ is usually called "gauge glass" model. It is expected on the basis of the analytical [2, 3, 4, 5] as well as numerical [6, 7] results that the gauge glass model in 3D space exhibits a true phase transition into a low-temperature glassy superconductive (nonergodic) state. The mean-field theory of such a low-temperature state shows [3, 5] that it is characterized by the presense of a finite effective penetration depth for the *variation* of an external field, nonzero macroscopic critical current, and the absense of a macroscopic Meissner effect. The full model (I.1) with α's containing contribution from $\mathbf{B}_{ind}$ is sometimes called "gauge glass with screening" [8]. The effect of screening on the presence and properties of the phase transition into a glassy state is not completely clear; some numerical results [8] indicate the absence of a true phase transtion in a 3D model with screening. Quantitatively, the strengh of screening is determined by the ratio $\beta_L = 2\pi\mathcal{L}I_c/c\Phi_0$ where $\mathcal{L}$ is the characteristic inductance of an elementary intergrain current loop [9]. In the ceramics with $\beta_L \ll 1$, screening effects become important on a long-distance scale $\sim a_0/\sqrt{\beta_L}$ only (i.e. they are similar to the strongly type-II superconductors with disorder).

Apart from its relevance for the description of granular superconductors, the gauge glass model with screening is rather often considered (e.g. Ref. [10]) as a simplified model describing the large-scale behaviour of disordered bulk type-II superconductors in the mixed state (so-called vortex glass problem). Actually it is unclear a priori how these two problems are related; an obvious difference between them is that the basic ingredient of the latter is the vortex lattice which is clearly

an anisotropic object, whereas the former does not contain any prescribed direction in the 3D space. On the other hand, the granular superconductor in a moderate magnetic field $H_{ext} \leq H_0$ may be considered as a kind of disordered type-II superconductor, where the notion of a hypervortex (which is the macroscopic analogue of the Abrikosov vortex) can be introduced [2, 11]. Therefore, the macroscopic properties of a granular network at $H_{ext} \leq H_0$ may resemble those of the vortex glass; in such a scenario a phase transtion between vortex glass and gauge glass phases would be expected in a granular superconductive network at $H_{ext} \sim H_0$ (cf. Ref.[1] for a more detailed discussion of this subject).

Recently, it was noted that granular superconductors may become glassy even in the absence of external magnetic field, if a large enough part of Josephson junctions are anomalous, i.e. their minimum Josephson coupling energy corresponds to a phase difference $\Delta\phi = \pi$ instead of 0 (so-called π-junctions). Two completely different origins of π-junctions were proposed: mesoscopic fluctuations in dirty superconductors [12] and the pairing with non-zero momentum [13, 14]. Recent experiments revealing the d-wave nature of pairing in high-temperature superconductors [15] indicate the possibility of observing glassy superconductive behaviour in HTSC ceramics in virtually zero magnetic field. Note that ceramics with equal concentrations of usual and π-junctions are completely equivalent (if screening effects can be neglected) to the XY spin glass. Contrary to the 3D gauge glass model, the XY spin glass in 3D is expected to have no true thermodynamic phase transition at finite temperature [7]; recently, it has been suggested that the XY spin-glass and d-wave ceramic superconductor might have a new equilibrium ordered phase, the so-called chiral-glass phase [16]. However, these issues are hardly relevant for the measurable response at temperatures much below "bare" glass transition temperature T_g, which we consider in this paper.

Experimental studies of granular superconductors reveal [9, 17] an appearance of magnetic irreversibility (a difference between Meissner and shielding magnetizations or, in other terms, between Field Cooled (F.C.) and Zero Field Cooled (Z.F.C.) magnetizations) below some temperature T_g, which is lower than the SC transition temperature T_c of the grains. However, detailed analysis of the magnetic response in such systems is usually complicated by the mixing of contributions from individual grains and from the intergrain currents. The goal of this paper is to develop a method which makes it possible to extract from the raw data on d.c. magnetic response the intergrain contribution and to compare its behaviour with existing theoretical predictions.

The compound $La_{1.8}Sr_{0.2}CuO_4$ was chosen in this study for experimental convenience, since its critical temperature ($\approx 32\,K$) is within the optimal temperature range of our noise and a.c. susceptibility measurements setup. The sample was fabricated by standard solid state reaction of La_2O_3, $SrCO_3$ and CuO [18]. Mixed powder was pressed into pellets which were sintered in air at 920°C for 12 hours. The material was then submitted to three cycles of regrinding, sifting to $20\,\mu m$, pressing and sintering again at 1100°C for 12 hours. Samples prepared in two successive runs were used in this study. In the first one (sample A), pellets $1\,mm$ thick and $10\,mm$ diameter were obtained, with a density about 80% of the theoretical bulk value. In the second one (sample B), cylinders of diameter $6\,mm$ and length 5 to $6\,mm$ were prepared with a density ratio about 88%. In both preparations, grains sizes were in the range 1 – 10 μm. Room temperature X-ray powder diffraction patterns showed the presence of a small amount ($< 5\%$) of the non superconductive compound $La_{1-2x}Sr_{2x}Cu_2O_5$.

The rest of the paper is organized as follows. In Section II the general analysis of the magnetic response data obtained on two different samples (A and B) of $La_{1.8}Sr_{0.2}CuO_4$ ceramics is presented and the intergrain (Josephson) contribution to the overall response is extracted. Section III is devoted to the detailed study of the magnetic response of Josephson intergrain network in the low-field range. It is found that the macroscopic critical current is suppressed considerably (by a factor 2), in a magnetic field of only about $2G$. The lower-field d.c.–response to field variations of order $0.05 \div 0.5G$ was analyzed for the F.C. states obtained at $H_{FC} = 0 \div 10G$ and two temperatures, $10K$ and $20K$. The data at $T = 10K$ and $H_{FC} = 0$ and $0.1G$ are shown to be compatible with the Bean critical-state picture [19] and the low-field critical current value is identified. The rest of the data are in a sharp contrast with Bean-model predictions: the screening current *grows sublinearly* (approximately as a square root) with increasing exitation field. Very low field, low frequency a.c. measurements are presented, which reveal the strongly irreversible nature of that anomalous response. A new phenomenological model is proposed for the treatment of these data. Its first predictions are found to be in a reasonable agreement with the data. In Section IV, the theoretical analysis of our experimental results is given in terms of the existing theories of "gauge-glass" state. It is shown that the observed transition temperature to the low-temperature state of the network and the magnitude of the (low-B, T) critical current are in sharp contradiction with the (usual) assumption that the zero-field granular network is unfrustrated. On the contrary, under the assump-

tion of a strongly frustrated network at $B = 0$, all basic measured parameters of the ceramic network are in mutual agreement. We believe that these estimates indicate the existence of a large proportion of π-junctions in the $La_{1.8}Sr_{0.2}CuO_4$ ceramics, possibly due to the d-wave nature of superconductivity in cuprates. The Section V is devoted to the development of a new model of diamagnetic response in glassy superconductors, which is necessary for the description of the anomalous data described at the end of Section III. This new model (in some sense, intermediate between the Bean [19] and the Campbell [20] ones) is based on two ideas: i) the existence of two characteristic "critical" currents (J_{c1} and $J_c \gg J_{c1}$), and ii) the fractal nature of free energy valleys in the ceramic network. Our conclusions are presented in Section VI, whereas some technical calculations can be found in the Appendix.

For convenience, the e.m.u system of units will be used for experimental data, and Gaussian units for the theoretical discussions.

II General Properties of D.C. Magnetic Response

The d.c. magnetization was measured by the classical extraction method. Two SQUID magnetometers were used: one a home made apparatus used in several previous spin-glass studies [21], the other a commercial system (Cryogenics S500).

In this section, we describe successively the static magnetic response of samples A and B and present a preliminary treatment of these data, in order to distinguish between the magnetic response of individual grains and intergrain currents [9, 22] (a detailed study of the latter is the subject of the next section). Firstly, we present results obtained after cooling the samples in various d.c. fields and applying small field increases. Secondly, we will derive from the results the response of the Josephson currents as a function of field and temperature. Finally, we will show that the behavior of the field cooled (F.C.) susceptibility can be satisfactorily accounted for if the system of Josephson currents does not carry Meissner magnetization. It will be shown that the same interpretation accounts fairly well for the F.C. results which, at first sight, are rather different for the samples A and B.

II-A Sample A

Sample A is a $1\,mm$ thick pellet with an approximately ellipsoidal shape of $2 \times 6\,mm$. Its calculated volume is $V \approx 8.5\,mm^3$ and the demagnetizing field coefficient for the field parallel to the longitudinal axis is $N \approx 0.06$ [23].

Figure 1: Magnetic moment of the sample A as a function of field applied in the zero field cooled state (e.m.u. units of moment correspond to $cm^3 - G$).

Fig. 1 displays the magnetic dipole moment of the sample cooled to $10\,K$ in zero field and submitted to cycles $0 \rightarrow H_{max} \rightarrow 0$ for several values of H_{max} up to $2\,G$. At the lowest increasing fields, the moment increases initially with a slope P_1. Above $1.5\,G$, it approaches a slope $P2$. The remanent positive moment saturates for $H_{max} \geq 1\,G$. The calculated moment of the sample for perfect volume shielding in an homogeneous field is (e.m.u. system):

$$\mathcal{M} = -\frac{H \cdot V}{4\pi(1-N)} = -0.72 \cdot 10^{-3} \times H\,cm^3\text{-}G\,.$$

Owing to the error in the evaluation of the volume, this value is determined with an accuracy of only $\pm 5\%$. Nevertheless, it is in fair agreement with the slope $P1$ in Fig. 1. On the other hand, the slope $P2$ is about 53%, a rather small value since the density ratio of the sample is about 80%. At such low temperatures (in comparison with $T_c \approx 32\,K$), where the lower critical field of the grain's material is above $100\,G$, one would expect expulsion of the field by the grains with a penetration depth λ. The expected value for the magnetization $M = \mathcal{M}/V$ of the system of uncoupled grains system can be calculated as [24]:

$$\frac{M}{H} = \frac{1}{4\pi} \cdot \frac{f}{1 - fN - (1-f)n} \qquad \text{(II.2)}$$

where f is the volume fraction of the superconductive material and n is the demagnetizing field for the

grains. For an estimate, we assume grains to be spherical ($n = 1/3$) and, using $M/H \approx 0.53 \cdot 1/4\pi$ and $N = 0.06$, we find $f \approx 0.41$. This value is considerably below the volume fraction of the sample filled by grains (≈ 0.8); we assume that the difference is due to the intergrain penetration depth λ being comparable to the grain size r and estimate an effective value of λ as

$$f = 0.41 = 0.8 \left(1 - \frac{\lambda}{r}\right)^3 \qquad \text{yielding} \qquad \lambda = 0.2\, r\,.$$

Taking an average size of $5\,\mu m$ for the grains, we obtain $\lambda \approx 500\,nm$. Values reported for the mean penetration depth in $La_{1.8}Sr_{0.2}CuO_4$ are about $200\,nm$ [25]. The value found here is larger than the expected mean value for the homogeneous material, indicating that the grains are not monocrystalline. This will be confirmed below by the results of field-cooling experiments.

Figure 2: Shielding susceptibiliy of the sample A as a function of temperature, normalized to the moment for complete shielding. Curves are arranged in the same ascending order as in the legend.

The shielding susceptibility is plotted in Fig. 2, as a function of temperature and for several values of the ambient F.C. field. The measurements were performed according to the following procedure: the sample was cooled in a field H_{dc} down to the working temperature and the moment was measured after waiting 300 sec; then the field was increased by a small amount $\Delta H \leq H_{dc}/10$ and the moment was measured again after waiting 300 sec. The figure displays the experimental shielding susceptibility normalized to the value for total shielding, i.e.:

$$\chi_{sh} = \frac{\mathcal{M}(H + \Delta H) - \mathcal{M}(H)}{\Delta H} \times \frac{4\pi(1-N)}{V}\,.$$

The curves show the double step usually ascribed to the action of both intragrain currents and Josephson intergrain currents [26]. At high temperature, the onset of grains diamagnetism occurs at about $32\,K$. Above $25\,K$, the response corresponds to the diamagnetism of the grains. At a fixed temperature, it is H_{dc} independent for $H_{dc} \leq 5\,G$, and decreases for increasing $H_{dc} > 5\,G$. Below $25\,K$, the onset of Josephson currents manifests as a second step of the diamagnetic response. This second step appears at a decreasing temperature as H_{dc} increases. At the lowest temperatures, the diamagnetic moment amounts to about 100% of flux expulsion at $H_{dc} = 0$ and decreases with increasing H_{dc}. At $H_{dc} > 8\,G$, the flux expulsion saturates at a value slightly above 50% which corresponds roughly to the level of 53% determined above for the grains response.

The susceptibility in Fig. 2 contains the contributions of grains and Josephson currents. The contributions can be separated on the line of the work by Dersh and Blatter [22]. The induction in the sample is given by $B = H + 4\pi(M_g + M_j)$ where M_g and M_j stand respectively for the magnetization of grains and of the Josephson currents. It should be noted that the magnetization due to macroscopic circulating currents in a superconductor is sample-size dependent, i.e. the corresponding susceptibility is not a local quantity. At the macroscopic scale of the circulating currents, the magnetization M_g can always be written as $\chi_g H_{local}$, where $\chi_g(H)$ is homogeneous over the sample. In what follows, we consider quantities averaged over the volume of the sample: in that case, M_j is the averaged moment per volume unit due to the currents. The demagnetizing field effect will be neglected in the calculations. We have verified that, owing to the small value of the demagnetizing factor , this does not modify the essential features of the result while allowing a simpler derivation (the effect of demagnetizing factor will be taken into account when analyzing the data from the sample B). We get $M_g = \chi_g(H + 4\pi M_j)$. Then $M = M_g + M_j = \chi_g H + M_j \mu_g$ (with $\mu_g = 1 + 4\pi\chi_g$), and

$$M_j = \frac{M - \chi_g H}{\mu_g}\,. \qquad \text{(II.3)}$$

Eq. (II.3) must be considered with care since χ_g is history and field dependent. In fact it is well-adapted to the description of the result of zero (or small) field cooling experiments. More generally, we must consider the response to field increments δH to obtain $\chi = \delta M/\delta H$. Then, the polarizability [27] χ_j of the Josephson network reads:

$$\chi_j = \frac{\chi - \chi_g}{\mu_g}\,. \qquad \text{(II.4)}$$

Note that we can equivalently consider the response of the currents system in an homogeneous medium with permeability μ_g. If the applied field is varied by δH, the Josephson network sees a variation of internal field $\delta H_i = \mu_g \delta H$ and develops a polarization $\delta M_j = \chi_j \delta H_i$. Then, we recover Eq. (II.4).

The value of χ_g could be determined in principle if we were able to obtain a packing of disconnected grains equivalent to the packing of the sintered sample. In practice this was not possible. Indeed, mechanical grinding resulted in breaking a large part of the grains and thus modifying the characteristics of the material. Nevertheless, it is possible to extract χ_g, at least approximately, from the data of Fig. 2. At high temperature, above the onset of intergrain currents at $\approx 25\,K$, the shielding susceptibility χ_{sh} is due to the grains alone, independent on H_{dc} below $\approx 6\,G$. At low temperatures, for H_{dc} above $\approx 6\,G$, the χ_{sh} curves superpose and there is no manifestation of the onset of intergrain currents. Thus , here also, χ_{sh} represents the response of the grains alone. Hence, the response χ_g of the grains can be reasonnably approximated by an interpolation between these two limits. The interpolation curve, obtained by a smoothing procedure between both curves at $H_{dc} = 0\,G$ and $H_{dc} = 20\,G$ is displayed on Fig. 2 (dotted curve). The values of χ_j derived from Eq. (II.4) are plotted versus temperature in Fig. 3, for $H_{dc} < 6\,G$.

Figure 3: Josephson currents susceptibility in the sample A as a function of temperature. Values have been calculated from data of Fig. 2 and using Eq. (II.4).

Note that the dependence of χ_j on H_{dc}, seen in the figure is supposed to reflect the behavior of the initial shielding properties of the Josephson network with the increase of H_{dc}. Nevertheless, non linearity of the response due to the correlative increase of the value of ΔH ($\Delta H = H/10$) cannot be excluded: this aspect will be studied in detail in sample B. Finally, one can note the similarity of our data with the results of earlier numeric simulations on a gauge glass system [17].

Above we have dicussed the system's responses to the variation of magnetic field at fixed temperature (i.e. shielding responses) and extracted from these data the polarizability χ_j of the intergrain system. Now we turn to the description of the results of the Field Cooling (F.C.) measurements. F.C. (Meissner) magnetization was measured by the standard procedure between $10K$ and $40\,K$ for fields from 0.01 to $20\,G$. The results are reported in Fig. 4 versus temperature and Fig. 5 versus applied field. Data are normalized to the value of the moment for 100% shielding.

Figure 4: F.C. (Meissner) susceptibility of sample A as a function of temperature for fields up to $20\,G$. Curves are arranged in the same ascending order as in the legend.

Even at the smallest field, the flux expulsion rate is no more than 45%, less than the 53% shielding by the grains. At low fields, below $1\,G$, there is an approximate affinity between the curves of M/H versus T. M/H can be extrapolated linearly to $H \to 0$. The result is plotted in Fig. 2 (solid circles): one can see that the extrapolated F.C. susceptibility superposes exactly with the low d.c. field shielding susceptibility above $25\,K$. Therefore, at low d.c. field above $25\,K$, the response of the grains system is reversible and it is well described by the low d.c. field shielding curves; this justifies the hypothesis used above for the calculation of χ_j. On the other hand (see Fig. 5), the behavior of the F.C. susceptibility as a function of H is not trivial. M/H decreases with increasing field and reaches a stable level (about 25% at

Figure 5: F.C. (Meissner) susceptibility of sample A as a function of field for selected temperatures Curves are arranged in the same ascending order as in tthe legend.

the lowest temperatures) at roughly $1\,G$. Whatever the temperature, this decrease is centered at a constant value of the field, about $0.1-0.3G$. Above $5G$, M/H decreases once more with increasing field. Note an essential difference between the F.C. results presented on Fig. 4 and the shielding results above (Fig. 2): the F.C. curves do not show any increase of the response M/H with the temperature decrease below 20K, where the intergrain coupling grows considerably (as it is seen from Fig. 2). This means that the network of intergrain currents does not produce Meissner (F.C.) magnetization, whereas it does produce *shielding* magnetization.

The behavior of the F.C. susceptibility $\chi_{FC} = M_{FC}/H$ as a function of the applied field H depicted in Fig. 5 shows two nontrivial features: i) crossover between two plateaus (at low and moderate values of H), which takes place between $0.1G$ and $1G$ independent of temperature, and ii) the value of the low-field χ_{FC} is noticeably lower than the Meissner response of uncoupled grains (45% versus 53%). These features can be understood in terms of (i), a polycrystalline structure of the grains, which can be suspected from the large values of the penetration depth obtained from the results of Fig. 1, and (ii), self-shielding (pinning of the magnetic flux) by the Josephson currents when lowering the temperature in an applied field.

We start from the feature i); the curves of F.C. magnetization in Fig. 5 are rather similar to those which were measured by Ruppel et al. [28] in YBaCuO ceramics. The authors interpreted their results on the basis of a theory of the flux expulsion by strongly anisotopic randomly oriented crystallites as derived by Wohllebeen et al. [29]. We stress that the model is not based on any activated flux creep mechanism. It is thus well-adapted to the analysis of our results: indeed, flux creep effects can hardly be invoked here since the temperature has no apparent effect of on the characteristic field related to the decrease of magnetization. The starting point of the model is that, provided the size b of the crystallites is such that $\lambda_{\|} \ll b \ll \lambda_{\perp}$, the longitudinal magnetization of a crystallite whose c-axis makes an angle α with the field is given by $M = -(H/4\pi)\cdot\gamma(\cos\alpha)^2$, where γ is a factor close to 1, depending on the ratio $\lambda_{\|}/b$. After averaging over α, one obtains $M/H = (\gamma/3)(1/4\pi)$. It must be stressed that the system of intragrain crystallites is a strongly-coupled system, contrary to the system of grains which composes the ceramic. Therefore, a grain consists of an ensemble of interconnected Josephson loops surrounding crystallites whose planes are nearly along the field and are thus transparent to the field. At low fields, this system will expel the flux with a penetration depth depending on the junction coupling energy. Nevertheless, when the field is such that a loop sees a flux larger than $\sim \Phi_o/2$, the macroscopic magnetization of the Josephson currents vanishes and the system reacts as an ensemble of disconnected crystallites [30]. The characteristic field of this crossover is such that [29]:

$$\frac{H_m s_c}{\Phi_o} \approx 0.1 \qquad \text{(II.5)}$$

Recently determined values for the penetration depth in $La_{1.8}Sr_{0.2}CuO_4$ [31] are $\lambda_{\|} = 150\,nm$ and $\lambda_{\perp} = 1500\,nm$. Older measurements indicate a higher anisotropy, up to a factor 14 [32]. We can thus reasonnably consider that the model can be applied in our case. Taking $H_m = 0.3\,G$, we obtain $s_c = 7.4\cdot 10^{-8} cm^2$. With $s_c \approx \pi b^2$ this leads to a mean diameter $b = 1.5\,\mu m$ for the crystallites. Above H_m, the system acts as an ensemble of crystallites whose average susceptibility is $(\gamma/3)(1/4\pi)$. With the density ratio $f = 0.8$, taking $\gamma = 1$ and supposing spherical crystallites we obtain from Eq. (II.2) $4\pi\frac{M}{H} = 0.31$ which is above the experimental value (the latter being about 0.25). Nevertheless, it must be noted that we have neglected here the effect of the factor γ and used a rather unrealistic spherical approximation for the shape of crystallites. Finally, it has been seen that above $5\,G$, the F.C. magnetization starts to decrease once more with increasing field although H_{c1} is larger than $100G$ in $La_{1.8}Sr_{0.2}CuO_4$. This can be due to intrinsic pinning inside the crystallites themselves when the applied field is such that the flux in the cross section of one crystallite is larger than Φ_o. With a mean radius of $0.8\,\mu m$ for the crystallites, this crossover occurs at about $10\,G$.

Now we turn to the discussion of the feature ii) mentioned above. At temperatures below $25\,K$, the Josephson currents become active. Their effect is that, at $10\,K$, the shielding response of the system of grains amounts at about 53%, while the F.C. susceptibility saturates at about 45%. This difference is enough to be significant and can be interpreted as the result of pinning by the Josephson network. In fact, this pinning can be understood as a back shielding effect of the Josephson currents against the decrease of local internal field, due to the temperature dependence of the grain's system permeability μ_g. We have seen above that the response of the system consists of the two parts: (i) for an applied field H, the internal field due to the grains seen by the intergrain currents is $H_i = \mu_g H$, and (ii) the intergrain currents system reacts to all variation of H_i with a polarizability χ_j and generates a magnetization $\delta M_j = \chi_j \delta H_i$. Thus, when the temperature is decreased by dT, the internal field decreases by $H\, d\mu_g/dT$ and the Josephson network tends to screen this variation. Since the intergrain currents give no Meissner effect, we consider their response as totally irreversible. Thus for a variation dT of the temperature, in a field H, the variation of induction is:

$$dB = (1 + 4\pi\chi_j) \left(\frac{d\mu_g}{dT}\right)_H H\, dT$$

On the other hand, $B = (1 + 4\pi\chi_{FC})\, H$. With $\mu_g = 1 + 4\pi\chi_g$, we finally obtain:

$$\chi_{FC} = \chi_g + 4\pi \int_{T_c}^{T} \chi_j \frac{d\chi_g}{dT}\, dT = \chi_g + \chi_j^{FC}. \qquad \text{(II.6)}$$

$M_j^{FC} = \chi_j^{FC} H$ is the magnetization produced by the Josephson currents due to variation of μ_g with decreasing temperature. As χ_g is known only in the limit $H_{dc} \to 0$, Eq. (II.6) has been used to calculate χ_{FC} versus T in the limit of low field. In order to do it, we started from the values of $\chi_g(H \to 0)$ as derived above; for χ_j, we have used the values given in Fig. 3 for the smallest field $H_{dc} = 0.06\,G$. The result is plotted on Fig. 6. The agreement of calculated values with experimental data is rather satisfactory, although not perfect.

This discrepancy is emphasized if Eq. (II.6) is reversed in order to calculate χ_j as a function of χ_g and χ_{FC}. The reason is that we have used here the simplest linear model of back shielding. In fact, as we will see later, the response of the currents system is strongly non-linear, with the susceptibility χ_j decreasing with increasing ΔH, and this effect becomes stronger as the temperature increases. The result is that the calculated efficiency of back shielding is underestimated, since the value of the experimental susceptibility is determined by applying finite increments ΔH.

Figure 6: χ_{FC} calculated with Eq. (II.6) from the values of χ_g and $\chi_j(0)$ (see text).

II-B Sample B

Sample B was machined from one of the original cylinders, in form of a parallelepiped of dimensions approximately $3 \times 3 \times 6\,mm^3$. Its calculated volume is $V \approx 52.6\,mm^3$ and its demagnetizing field coefficient for a longitudinal field is $N \approx 0.19$. In a longitudinal field, its calculated moment for perfect flux expulsion is given by $\mathcal{M} = 5.1 \pm 0.2 \cdot 10^{-3} \times H\ cm^3$-$G$

Measurements of the initial magnetization at $10\,K$ are in fair agreement with this value. For H_{dc} above $3\,G$ and up to $30\,G$ $\Delta\mathcal{M}/\Delta H$ reaches a stable level about $3.2\,10^{-3}\,cm^3$ which corresponds to the response of the grains alone. With the density ratio of 88% for this sample and using Eq. (II.2) one finds $f = 0.46$, yielding $\lambda = 0.19\,r$, i.e. the same value as derived for sample A.

The shielding susceptibility was measured in this sample by using a more sophisticated method, in order to reduce the effect of non linearity. After cooling the sample at the working temperature in the d.c. field, the field was increased by 5 successive steps ΔH, and $\Delta\mathcal{M}$ was measured. At the lowest fields, $\Delta H = 10\,mG$ and (to keep a good signal/noise ratio) $\Delta H = H_{dc}/50$ at the highest ones. Then, the value of $\Delta\mathcal{M}_n / \sum_n \Delta H$ was extrapolated to $\Delta H = 0$ by least square fit.

Like in the case of sample A, all curves at $H_{dc} \leq 10\,G$ merge at high temperatures to a common curve which corresponds to the flux expulsion by the grains. The main difference with the sample A is that in the sample B the onset of Josephson currents shielding occurs at higher temperatures. This is consistent with the fact that sample B is more dense, resulting in a better cou-

pling between grains; moreover, its size is larger, which also increases the total shielding magnetization. At low temperature, the magnetization curve at $H_{dc} = 20\,G$ reaches a level slightly above 60%, which corresponds to the low temperature level for the grains.

The shielding response of the Josephson currents is obtained with the procedure already used for the sample A. Here the demagnetizing factor cannot be neglected ($N \approx 0.19$). Two kind of quantities are to be considered: (i) the responses χ_g and χ of an equivalent sample without demagnetizing field (e.g. an infinitely long cylinder with the same cross-section for instance); here χ_g is the response of the system of grains alone, without intergrain currents, and χ is the total response of the system of intragrain plus intergrain currents, and (ii), the measured responses $\overline{\chi}_g$ and $\overline{\chi}$; they correspond to the measured moment for each case, normalized to the moment for total flux expulsion in the volume of the sample. The relation between both kinds of quantities is given by $\frac{M}{H} = \frac{\overline{\chi}}{1-N} = \frac{\chi}{1+4\pi N\chi}$. A relation of the same kind holds for χ_g and $\overline{\chi}_g$. With the use of Eq. (II.4), we finally obtain:

$$\chi_j = \frac{\overline{\chi} - \overline{\chi}_g}{(1 - N\overline{\mu})\ \overline{\mu}_g} \qquad \text{(II.7)}$$

where $\overline{\mu} = 1+4\pi\overline{\chi}$, $\overline{\mu}_g = 1+4\pi\overline{\chi}_g$. Similar to the case of the sample A, an approximate curve has been determined for $\overline{\chi}_g$ by interpolating between the small H_{dc} curves at high temperatures, and the curve at $H_{dc} = 20\,G$ at low temperatures. Then the values of χ_j have been derived from Eq. (II.7) and plotted on Fig. 7. The set of curves is similar to the set for sample A, except for the higher onset temperature of the intergrains currents.

Figure 7: Josephson currents shielding susceptibility as derived from the data and use of Eq. (II.7).

Field Cooled magnetization data, normalized to the value of the moment for full flux expulsion, are reported in Fig. 8 as a function of fields up to $30\,G$.

Figure 8: F.C. (Meissner) susceptibility of sample B normalized to the moment for total flux expulsion, as a function of field.

At the lowest field and temperature, the F.C. magnetization does not exceed 28% of its value for full flux expulsion. Furthermore, at low temperatures the curves versus field present a second maximum at about $5\,G$. We expect that this complicated behavior is due to the back shielding effect of the intergrain currents, as discussed for sample A. To take them into account, a relation similar to Eq. (II.6) (but with the demagnetizing effect taken into account) should be derived. The internal field is given as usual by $H_i = H - 4\pi NM$, and the value of the local field seen by the currents is $H_l = \mu_g\, H_i$. Thus, under a temperature variation dT,

$$\frac{dH_l}{dT} = \frac{d\mu_g}{dT}\,(H - 4\pi NM)\ -\ 4\pi N\ \mu_g\,\frac{dM}{dT}\,.$$

With $dB/dT = \mu_j\, dH_l/dT$, and using the relation

$$M = \frac{\overline{\chi}_{FC} H}{1-N} = \frac{1}{4\pi}\ \int_{T_c}^{T} \frac{d(B - H_i)}{dT}\, dT$$

one obtains after integration:

$$\overline{\chi}_{FC} = \frac{1-N}{4\pi N}\,(1 - \exp{(-4\pi NI)})\,; \qquad I = \int_{T_c}^{T} \frac{\mu_j}{1 - N\ (1 - \mu_g\ \mu_j)} \qquad \text{(II.8)}$$

Here $\mu_j = 1 + 4\pi\chi_j$, with χ_j reported on Fig. 7, whereas the value of μ_g was obtained using the relation $\mu_g = (1 - N)\overline{\mu}_g/(1 - N\overline{\mu}_g)$ from the value of $\overline{\chi}_g$ as derived above.

The values of $\overline{\chi}_{FC}$ for $H \to 0$ have been calculated using the values of $\overline{\chi}_g$ as determined above, and the values of χ_j at $H_{dc} = 0$. The calculated value of $\overline{\chi}_{FC}$ was found to be about -0.35 at $T = 10K$, whereas its measured value was about -0.28. The discrepancy between measured and calculated values is larger here than in corresponding results for sample A. We believe that the origin of this discrepancy is the same as in the case of sample A, i.e. it stems from the nonlinear response effect. This effect is numerically larger in sample B since here the onset of Josephson currents occurs in a range of temperature where χ_g still varies strongly, contrary to the case of sample A.

The above analysis shows (irrespectively to the abovementioned discrepancy) that the back shielding effect leads to a strong reduction of the field cooled susceptibility as compared with the susceptibility of the grains alone. It is then easy to understand the complex behavior of $\overline{\chi}_{FC}$ as a funtion of field: at $10\,K$ for instance, the onset of back shielding occurs at about $20\,G$, and its amplitude increases with decreasing field due to the increase of $\overline{\chi}_j$. Starting from the two-step behavior of χ_g expected from the theory of Wohllebeen et al. [29] (and seen in the data of sample A, where back shielding is less important), back shielding results on the double maximum shape of the measured curves.

III Detailed Study of the Josephson Network Response.

III-A Determination of the global critical current.

In this subsection we will present the procedure we used to extract the value of the macroscopic critical current in our sample B. This procedure is not quite trivial since we are interested in the dependence of the critical current on the background d.c. field in the sample, so we need to analyse the magnetization curves which depend both on the cooling field $H_{d.c.}$ and on the field variation δH.

Magnetization has been recorded at 10 and $20\,K$ as a function of increasing ΔH with the smallest possible field steps ($\delta H = 10\,mG$), and starting from several F.C. states. From the $\Delta\mathcal{M}$ data, it is possible to derive the value of the current response $\Delta\mathcal{M}_j$ as a function of ΔH. For this, we use Eq. (II.7) which can be written as :

$$\Delta\mathcal{M}_j = \frac{\Delta\mathcal{M} - \Delta\mathcal{M}_g}{(1 - N\overline{\mu})\,\overline{\mu}_g}\,. \qquad \text{(III.9)}$$

where $\Delta\mathcal{M}_g$ is the magnetization of the grains alone; $\overline{\mu}$ and $\overline{\mu}_g$ are defined in Section II-B. The value of the grains system response is approximately derived in the same section: $\Delta\mathcal{M}_g \approx 3.2\,10^{-3} \times H\,cm^3 - G$ at $10\,K$ and $\Delta\mathcal{M}_g \approx 2.9\,10^{-3} \times H\,cm^3 - G$ at $20\,K$. Calculated values of $\Delta\mathcal{M}_j$ at $10\,K$ are plotted in Fig. 9. Note the analogy of these results to the magnetization curves of classical type II superconductors with strong pinning (the difference is that here ΔH plays the role of H).

Figure 9: Shielding moment of the Josephson currents after cooling the sample at $10\,K$ in a d.c. field in the range $0 - 10\,G$.

After cooling the sample at zero d.c. field, its response is obviously symmetric with respect to ΔH. When it is cooled in a finite d.c. field, it is not the case anymore, as was explained in the previous section. The magnetic moment of the sample just after cooling is $\mathcal{M}_{FC} = \mathcal{M}_g + \mathcal{M}_j^{FC}$ where $\mathcal{M}_j^{FC}$ is the positive moment due to the back shielding by the Josephson currents which have been developed during the cooling process (see Eq. (II.4 and II.7)). So, the total moment produced by the intergrain currents after increasing the field by ΔH is $\mathcal{M}_j = \mathcal{M}_j^{FC} + \Delta\mathcal{M}_j$. It is this moment which vanishes when $J_c \to 0$ (at large enough ΔH), and thus $\Delta\mathcal{M}_j$ approaches $-\mathcal{M}_j^{FC}$. In Fig. 10 we show the data recorded at $T = 10\,K$ and $H_{dc} = 2\,G$. Curves recorded at positive and negative ΔH both converge to the value corresponding to $-\mathcal{M}_j^{FC}$: at $10\,K$, $-\mathcal{M}_j^{FC}$ is about $1.1\,10^{-3} emu$.

When $\Delta H > H_{dc}$, it is natural to expect that the response of the Josephson network does not depend on the initial state. A simple illustration can be given by analogy with Bean-like pinning in type II superconductors [19]. At large ΔH, when the induction profile has penetrated up to the center of the sample, the magnetization no longer depends on ΔH but only on J_c. If, as it

Figure 10: Shielding moment of the Josephson currents after cooling the sample at $10\,K$ in a d.c. field $H_{dc} = 2\,G$. Data are for positive and negative field steps.

is the case in real materials, J_c varies with the induction in the sample, the magnetization depends on the total H, whatever the value of H_{dc} in which the sample was cooled. Actually, when plotted as a function of the total field $H_{dc} + \Delta H$, the curves giving the total moment of network currents $\mathcal{M}_j^{FC} + \Delta\mathcal{M}_j$ merge in their "large" field part (i.e. above their maximum). The values have been calculated, with $-\mathcal{M}_j^{FC} = 1.1\,10^{-3} emu$ and $0.7\,10^{-3} emu$ for $H_{dc} = 2\,G$ and $4\,G$ respectively. In order to obtain an optimal overlap between the curves, the following values have been used for $\Delta\mathcal{M}_g$: $3.25\,10^{-3} \times H\,cm^3 - G$ at $H_{dc} = 0\,G$, $3.22\,10^{-3} \times H\,cm^3 - G$ at $H_{dc} = 2\,G$ and $4\,G$. Indeed, the calculated values for $\Delta\mathcal{M}_j$ at large ΔH are extremely sensitive to those for $\Delta\mathcal{M}_g$. This allows us to refine the determination of $\Delta\mathcal{M}_g$. Note that the values quoted above do not differ by more than 1%, which is compatible with experimental accuracy and the possible variations of grains response with H_{dc}.

Finally, from the knowledge of the true Josephson shielding response, in "large" fields we can now derive a rough evaluation of the critical current. Namely, above the maximum of $\Delta\mathcal{M}_j$, we calculate the value $\tilde{J}_c$ of the average critical current which would give the value of the measured moment by use of the Bean formula [19] in a cylindrical geometry. For strong penetration, the magnetization is given in e.m.u. by $M = \tilde{J}_c R/3$. With $R = 0.15\,cm$ and the values of the moment measured at $10\,K$ and $20\,K$ with $H_{dc} = 0\,G$, we obtain the data displayed in Fig. 11. Note that the data are limited to fields such that $H \approx H^* = 4\pi\tilde{J}_c R$ below which the above approximate evaluation is no longer relevant.

Figure 11: Calculated values of the averaged critical current $\tilde{J}_c$ as a function of total field for strong field penetration. The big square corresponds to the initial J_c as determined in III-B

III-B Low Field d.c. Response.

We can now concentrate on the behavior of the Josephson currents moment at small ΔH. For this discussion, the currents susceptibility $\Delta\mathcal{M}_j/\Delta H$ is plotted versus ΔH at $10\,K$ and $20\,K$ in Fig. 12 and 13, respectively.

At $10\,K$, after zero field cooling or cooling in a small field $H_{dc} = 0.1\,G$, the response varies linearly with ΔH for small values of ΔH up to about $0.5\,G$. This linear slope of $\Delta\mathcal{M}_j/\Delta H$ is considered as the result of classical Bean-like pinning with critical current density $J_c = H^*/4\pi R$, where $1/4\pi H^*$ is the initial slope of the curve [19]. This initial slope is reported on the figure as the short dashed line which corresponds to $H^* = 2\,G$, leading to $J_c \approx 3.7 A/cm^2$.

At larger ΔH, the behaviour of currents susceptibility $\Delta\mathcal{M}_j/\Delta H$ deviates from linear, which is the result of both the magnetic-field dependence of the critical current J_c, an intrinsic effect, and of the increasing degree of flux penetration into the sample , a purely size-dependent effect. Usually one uses the Bean model (generally with some B-dependent critical current) in an appropriate geometry in order to deconvolute these two effects. However, one should keep in mind that the Bean model is a severe simplification of the problem of constant pinning force, corresponding to the limit $\lambda \to 0$ (i.e. the London penetration depth is supposed to be negligible with respect to the Bean penetration

Figure 12: Josephson currents susceptibility at $10\,K$ vs. applied variation ΔH of field, after cooling in d.c. field H_{dc}. The meaning of dashed and dot dashed lines is explained in the text.

Figure 13: Josephson currents susceptibility at $20\,K$ vs. applied variation ΔH of field, after cooling in d.c. field H_{dc}.

length). For the simplest sample shapes (thin slab or cylinder) it means that the condition $\lambda \ll R$ should be fulfilled, which is usually the case. However the situation is more complicated for samples of square cross-section (like our one), where the effect of corners may become important even at $\lambda \ll R$. For such a geometry, the use of Bean model leads to exactly the same relation between critical current, external field and measured magnetization as for the cylindrical ones, whereas one expects some difference if finite-λ corrections are taken into account. At the present stage, we are not able to evaluate these corrections and therefore the values of the magnetization corresponding to our experimental geometry with non negligible λ. Nevertheless, we expect that it lies between the curves for two extreme limits. The upper one corresponds to the $\lambda \to 0$ limit, where the magnetization is given simply by the Bean's formula for the cylinder: $4\pi M/H = -1 + H/H^* - H^2/3H^{*2}$ for $H < H^*$ and $4\pi M/H = -H^*/3H$ for $H > H^*$. A lower limit (thought rather artificial) consists of the "double slab" case in which the variation of magnetization is counted twice (once for each pair of edges): $4\pi M/H = -1 + H/H^*$ for $H < H^*/2$ and $4\pi M/H = -H^*/4H$ for $H > H^*/2$. Both curves are plotted in the Fig. 12 (dot dashed and long dashed curves respectively) for $J_c = 3.7 A/cm^2$ and $\Delta\mathcal{M}_j/\Delta H = -5.05\,10^{-3} cm^3$ at $\Delta H \to 0$.

Let us now discuss the data starting from those obtained for low d.c. fields, $H_{d.c.} = 0, 0.1\,G$. One can see that, after the initial linear part, the absolute value of the measured susceptibility is always smaller than the calculated ones. This corresponds to the decrease of J_c with increasing induction, as it is classically expected in granular materials, due to the suppression of intergrain critical currents by magnetic field penetration into the Josephson junctions[9]. This "classical" behavior for granular superconductors is usually analyzed by considering the volume-averaged Josephson medium as a kind of type II superconductor in the dirty limit, provided its macroscopic penetration depth λ_J is large as compared with the grains size [11, 35].

At $H_{dc} \geq 2\,G$ the behavior of $\Delta\mathcal{M}_j/\Delta H$ is quite different: there is no initial linear slope, but a monotonic curvature is present down to the smallest ΔH. It is no longer possible to adjust a Bean like curve to the data. For instance, the Bean curve plotted on the lowest ΔH data for $H_{dc} = 2\,G$ is reported on the Fig. 12 as a dashed line. It corresponds to a very small critical current of order $0.2\,A/cm^2$, and it is evident that the effective screening current becomes much larger with increasing ΔH. Here, contrary to the case of $H_{dc} = 0G$, the absolute value of the measured susceptibility is always

larger than the calculated one for a constant shielding current corresponding to the limit $\Delta H \to 0$. This means that, whereas at $H_{dc} = 0$ the effective screening current density stays constant and then slowly decreases with increasing ΔH (which corresponds to classical Josephson pinning), at $H_{dc} \geq 2\,G$ it *increases* with ΔH *sublinearly* (since a linear increase would correspond to a susceptibility independent of ΔH). Such behaviour is quite unusual within the commonly accepted picture of screening in superconductors; indeed, we know that, for vanishing field excitations, the screening current may be either i) *linear* in ΔH and *reversible*, as in the London (or Campbell [20]) shielding regime, or ii) *constant* (equal to the initial critical current J_c) and *irreversible* as in the case of the Bean-type critical state (or of any other known critical model, e.g Kim model [33], exponential model [34], etc).

The above anomalous screening behaviour is even more pronounced at $20\,K$ where, even after zero field cooling, no initial linear slope of $\Delta\mathcal{M}_j/\Delta H$ can be seen in the data. All curves show the same anomalous behavior as the data at $10\,K$ in fields from $2\,G$. This specific behavior is emphasized by plotting the difference between the measured susceptibility $\Delta\mathcal{M}_j/\Delta H$ and its value for total flux expulsion $\Delta\mathcal{M}_j(0)/\Delta H$, versus ΔH on a Log–Log scale. In such a plot, at least in the regime of weak penetration, i.e. where $\Delta\mathcal{M}_j/\Delta H$ is larger than $0.8\,\Delta\mathcal{M}_j(0)/\Delta H$, sublinear variation of the shielding current density results in a logarithmic slope smaller than 1 for the curves of $\Delta\mathcal{M}_j/\Delta H$ (for $\Delta\mathcal{M}_j/\Delta H$ smaller than $0.8\,\Delta\mathcal{M}_j(0)/\Delta H$, we are in a regime of strong penetration where it is no longer possible to relate simply the variations of the moment response to those of the shielding current). In Fig. 14, we have reported the three curves for which data are found in the range above $0.8\,\Delta\mathcal{M}_j(0)/\Delta H$, i.e. at $T = 10\,K$, $H_{dc} = 0\,G$ and $2\,G$, and $T = 20\,K$ $H_{dc} = 0\,G$.

At $10\,K$ and $H_{dc} = 0\,G$, the logarithmic slope is about 1 as expected, although at the smallest fields the curve crosses over to a smaller logarithmic slope closer to 0.5. At $20\,K$ and $H_{dc} = 0\,G$ the logarithmic slope is about 0.4 at the lowest ΔH. Approximately the same value of the slope characterizes the data obtained at $10\,K$ and $H_{dc} = 2\,G$, although the dispersion of data points at lowest ΔH makes its accurate determination difficult.

The above anomalous behaviour makes it tempting to try a simple *Ansatz* for the behavior of the response current density of the system versus induction variations. Let us suppose that $J \propto \Delta B^{\alpha}$ with α between 0 and 1. The case with $\alpha = 1$ corresponds simply to classical screening with penetration length λ (since $J \propto \Delta B$); the case with $\alpha = 0$ corresponds to constant J, i.e. the classical Bean case. Anomalous response arises for non integer α. For very small excitation ΔH, the length of induction penetration is small as compared with the size of the sample and we need to consider the effect of the excitation in the lowest order in ΔB only. For the purpose of illustration we consider the simplest slab geometry. Then the induction profile is determined by the Maxwell equation

$$\frac{dB}{dx} = -4\pi J_1 \left(\frac{\Delta B}{\Delta B_1}\right)^{\alpha} \qquad \text{(III.10)}$$

where x is the coordinate perpendicular to the edge of the sample. For an external field ΔH, the induction in the sample is given by

$$\Delta B(x) = \left(\frac{(1-\alpha)4\pi J_1}{{\Delta B_1}^{\alpha}}\,(x_H - x)\right)^{1/(1-\alpha)} \qquad \text{(III.11)}$$

where x_H is the coordinate of penetration and J_1 and ΔB_1 are normalizing factors; for $x = 0$, $\Delta B = \Delta H$, i.e. $x_H = {\Delta B_1}^{\alpha}/(4\pi J_1(1-\alpha)) \cdot \Delta H^{1-\alpha}$. Then, integrating the field profile (III.11) over x, we get

$$\frac{4\pi\Delta\overline{M} + \Delta H}{\Delta H} \propto \Delta H^{1-\alpha}, \qquad \text{(III.12)}$$

where $\Delta\overline{M} = \Delta\mathcal{M}/V$ is the mean magnetization variation due to the field variation ΔH.

If we now compare the result (III.12) with the data shown in Fig. 14, we find values of α in the range $0.4 \div 0.5$ at both $10\,K$ and $20\,K$.

Figure 14: Difference between the measured susceptibility and its value for perfect shielding for selected data at $10\,K$ and $20\,K$. The short dashed line represents a logarithmic slope 1 expected for a Bean critical state.

Thus a simple choice for the relation between the screening current J_c and the induction variation ΔB allows us to imitate the experimental results for the simplest protocol of a weak monotonic ΔH variation on top of a homogeneous state of the network. Nevertheless, it is evident that ΔB has no clear meaning if the variation of H is non-monotonic or if the initial state is obtained by non-zero field cooling. Indeed, in the later case, induction in the sample varies during cooling due to the variation of μ_g with T, giving the response $\Delta\mathcal{M}_j^{FC}$ as seen before. Furthermore, we will see below that the response is irreversible even for extremely low exitation fields.

III-C Irreversibility: Very Low Field, low Frequency a.c. Response.

Problems of sensitivity limit the range of small excitations which can be used in d.c. experiments. The preceding results clearly show the sublinear nature of the low field response, but they do not allow its precise determination. In order to extend by several orders of magnitude the range of our lower excitations investigation, we have been led to perform a.c. susceptibility measurements. The use of a.c. response measurements is always questionnable when equilibrium (or quasi-equilibrium) properties are under investigation, since the results can be affected by the time-dependent part of the response function. It has been shown that the latter is the response of a very good conductor with complex conductivity [36, 37]. Hence, it is necessary to work at low frequency, in a range where the susceptibility is roughly frequency independent.

We present here preliminary results obtained on a long cylinder obtained by stacking several of the original sample B cylinders. Measurements were done at $20\,K$, at a working frequency of $1.7\,Hz$ in the equipment used for noise experiments [37]. The sample was simply shifted into the upper half of the third order gradiometer. At this temperature and frequency, we have verified that the in-phase susceptibility is almost frequency independent, which ensures that the results are mainly dependent on the (quasi) static part of the response. The susceptibility was recorded using classical method of SQUID magnetometry. We used a.c. excitation fields in the range $3\,10^{-2}$–$30\,mG$ and the sample was cooled in d.c. fields from 0 to $8.8\,G$. From the data, the values of the Josephson network susceptibility was extacted using the method developed in Section II, with the susceptibilities in Eq. (II.7) being complex quantities. The susceptibility measured at $4.2\,K$ at the lowest a.c. amplitude was taken as the level for perfect diamagnetism. Fig. 15 displays a log-log plot of the out-of-phase susceptibility χ_j'' versus the amplitude of the a.c. field, and for several values of the F.C. static field. The response is irreversible down to the lowest a.c amplitudes, and the irreversibility increases with the superimposed d.c. field. All curves follow a power law , with the same exponent close to 0.5. Going towards the smallest a.c. excitations, they show some downward bend which could be related with the approach to a linear regime (with $\chi_j'' = 0$) below $0.1\,mG$, although the dispersion of the data is too high to conclude. The in-phase susceptibility χ_j' is plotted as a function of $H_{ac}^{0.5}$ in Fig. 16. Here as well, the anoma-

Figure 15: Out-of-phase susceptibility at $1.7\,Hz$ as a function of a.c. field amplitude.

Figure 16: In-phase susceptibility at $1.7\,Hz$ as a function of the power of a.c. field amplitude $H_{ac}^{0.5}$.

Figure 17: Plot of $4\pi\chi_j''$ as a function of $1+4\pi\chi_j'$ for the different values of H_{dc}.

lous nature of the response is clearly seen. $4\pi\chi_j'$ behaves like $(-1+\delta+\gamma H_{ac}^{0.5})$ where both the constant δ and the slope γ increase with increasing superimposed static field H_{dc}. The dependence of the harmonic susceptibility on the a.c. field amplitude is a genuine proof of the existence of static irreversibility in the response. This is not astonishing by itself, but these results stress the anomalous aspect of this irreversibility. For instance, in the classical Bean case with a weak penetration, it is known that $1+4\pi\chi_j'$ and χ_j'' are proportional to H_{ac} whereas Fig. 15 and 16 clearly show the proportionality to $H_{ac}^{0.5}$. A further evidence is provided by plotting χ_j'' versus $1+4\pi\chi_j'$ as displayed in figure 17. It can be shown that if the a.c. response is driven only by static irreversibility, both are proportional. In the Bean case, the coefficient of proportionality is $4/3\pi$. In the figure 17, the part of data which lie in the range of 20% variation of χ_j' (where the relations for slab geometry are approximately valid) show that χ_j'' is indeed proportional to $1+4\pi\chi_j'$, but with a bit smaller coefficient $\approx 0.28 \pm 0.03$.

In order to understand the meaning of the above results, we generalize the crude *ad hoc* model of Section III-B to the irreversible case. In order to do it, we generalize the protocol of the Bean model. Namely, in the Bean model, the current is given by a step function of the variation of induction, $J = J_c sgn(\Delta B)$ according to the sign of ΔB, as long as the induction variation is monotonous. If the sign of variation of B is reversed, J also changes sign, which can be written in terms of the *variation* of the current density (with respect to the initial current distribution obtained after monotonous variation of the field, J_{init}, $\Delta J = -2J_{init}\Theta(-\Delta B_{new})$ where $\Theta(x) = (1/2)(1+sgn(x))$ and $\Delta B_{new} = B - B_{init}$. Such a representation (which is not needed in the analysis of the Bean model itself) will allow us to construct the necessary generalization of the relation between current and variation of the field used in Eq.(III.10). Actually our goal here is rather limited: we are going to find a consistent description of the simplest hysteresis cycle which consists of the initial increase of ΔB from zero to ΔB_{init}, then reversing the sign of the field variation until the value of $\Delta B = -\Delta B_{init}$ is reached, and then reversing dB/dt once more and finishing at $\Delta B_{final} = \Delta B_{init}$. The description of this cycle will be consistent if we find that the value of the current density at the end-point, J_{final}, coincides with the one after the original increase of the field ΔB_{init}, J_{init}. This simply means that the hysteresis loop is closed. It is easy to check that the above condition will be fulfilled by the following choice of the $\Delta J(\Delta B_{new})$ dependence:

$$\Delta J = -sgn(J_{init}) 2^{1-\alpha} J_1 \left(\frac{\Delta B_{new}}{\Delta B_1}\right)^{\alpha} \Theta(-\Delta B_{new}) \,. \tag{III.13}$$

where J_1 and ΔB_1 have the same meaning as in Eq.(III.10). Actually the only difference between the Eq. (III.13) and the original used in the Eq.(III.10) is the coefficient $2^{1-\alpha}$. The Bean model limit then corresponds to $\alpha \to 0$, so the above coefficient approaches 2 as it should. Then instead of Eq. (III.10) we obtain:

$$d\Delta B/dx = \pm 2^{1-\alpha} \mathcal{A}\, \Delta B^{\alpha} \tag{III.14}$$

where $\mathcal{A} = 4\pi J_1/\Delta B_1^{\alpha}$. The induction profile, induced magnetization and harmonic response are calculated in the Appendix. The main conclusions are that the fundamental components $1+4\pi\chi_j'$ and χ_j'' are both proportional to ${h_o}^{1-\alpha}$, and that their ratio $R = \chi_j''/(1+4\pi\chi_j')$ decreases from $4/3\pi$ to 0 when α goes from 0 to 1. For $\alpha = 0.5$, we get (cf. Fig. 21) $R \approx 0.25$, a value which is in good agreement with the data presented on Fig. 17. Note that the degree of irreversibility (measured by this ratio) is similar (although a bit lower) to the one of the Bean model. It should be emphasized that the numerical coefficient in Eq. (III.13) was "fitted" in order to obtain consistent (i.e. closed) hysteresis loop; one can expect that an analogous equation describing current variation after some more complicated history of the field variations will contain another (history-dependent) numerical coefficient instead of $2^{1-\alpha}$.

It can be seen from Figs. 15 and 16 that $\mathcal{A} = 4\pi J_1/\Delta B_1^{\alpha}$ increases with increasing ambient d.c. field. It is natural to expect a decrease of J_1 with increasing H_{dc}. The increase of $\mathcal{A}$ with H_{dc} means that ΔB_1^{α} decreases more quickly than J_1 when H_{dc} increases. The

presence and behavior of the constant δ cannot be predicted on the basis of the above simple model. In fact, the latter neglects the possibility of elastic displacement of flux lines under the action of the external applied field. Such an effect would result in a response analogous to the Campbell response due to the elastic displacement of vortices in their pinning potential in type II superconductors [20]. Campbell's response is linear, so it would result in an a.c. field independent positive contribution to χ', whose amplitude would be inversely proportional to the strength of the restoring force of the pinning potential wells. It is natural to expect that the pinning force decreases with increasing ambient d.c. field in our granular system, due to the reduction of the junctions critical currents. Hence, such an effect would give a positive contribution to χ', which would increase with increasing d.c. field. This corresponds rather well to the behavior of the offset δ seen in the data.

IV Comparison with an existing theory of gauge glass: frustration at $H = 0$

In this Section we compare the experimental results described above with the theoretical results available for the randomly frustrated Josephson networks. We start from a simple estimate for the mean energy $E_J = \hbar I_c/2e$ using the experimental value of the low-temperature, Z.F.C. ($T = 10K, H_{dc} = 0$) critical current density $J_c \approx 3.7A/cm^2$. Using the estimate $a_0 \approx 5\mu m$ for the mean size of the grains, one could naively obtain $I_c \approx J_c a_0^2 \approx 1\mu A$ and the corresponding low-temperature Josephson energy $E_J^{naive} \approx 20K$ (this value was derived from J_c measured at $T = 10K$, but we do not expect much difference in the intrinsic Josephson energies at $T = 10K$ and at $T \to 0$ since the bulk transition temperature in $La_{1.8}Sr_{0.2}CuO_4$ is $T_c \approx 32K$). However such an estimate is in contradiction with the measured value of the glass transition temperature $T_g \approx 29K$. Indeed, let us assume that the mean coordination number (number of "interacting neigbours") Z in the ceramics is around 6, as for a simple cubic lattice. Then for the estimate of the relation between E_J and T_g one can use the simulation data [6, 7] which give $T_g \approx 0.5E_J(T_g) = 0.5E_{J_o}\cdot(1-T_g/T_c)$, where we took into account the linear dependence of E_J on $T_c - T$ close to the bulk transition temperature. As a result, one gets

$$\frac{E_{J_o}}{k_B} \approx \frac{2T_g}{1 - T_g/T_c} \approx 600K \qquad \text{(IV.15)}$$

i.e. a factor 30 larger than the naive estimate above. However we will show now that this discrepancy may be resolved if we assume that the current network producing the measured critical current density J_c was actually *strongly frustrated* in spite of the absence of background d.c. field in this measurement.

The macroscopic critical current density J_c for a strongly frustrated Josephson network was calculated in Ref. [5] within the mean-field approach (we are not aware of any calculations of this kind beyond the scope of the mean-field theory). It was shown that frustration strongly reduces J_c as compared to its value J_0 for an unfrustrated system, $J_c/J_0 = \frac{3\sqrt{3}\gamma}{8}(1 - T/T_g)^{5/2}$, where the factor $\gamma \approx 0.065$ was obtained by numerical solution of the *slow cooling* equations [3, 38, 39] describing the evolution of the glassy state under slow variations of temperature and magnetic field. In the low-temperature limit, this relation amounts to a factor 25 reduction of the J_c value with respect to J_0. Correspondingly, the characteristic value of the critical current for an individual junction will be obtained as $I_c \approx 25 J_c a_0^2 \approx 25\mu A$ and results in a Josephson coupling energy $E_{J_o} \approx 500K$, in a fairly good agreement with the above estimate (IV.15).

The above estimates show that the network of Josephson junctions in $La_{1.8}Sr_{0.2}CuO_4$ is frustrated even in the absence of an external magnetic field. A careful reader could question this conclusion since we have used some results from the mean-field theory which may be a poor approximation for a 3D gauge-glass. We believe, however that the qualitative result of the above estimates is sufficiently robust because a strong reduction of J_c with respect to J_0 should be a general feature of a glassy network, so that unaccuracy due to mean-field approximation cannot compensate for a huge discrepancy obtained between E_J^{naive} and the estimate (IV.15). Additional evidence in favor of the glassy nature of our system is provided by the similarity of the low-ΔH diamagnetic response at $T = 20K$ with zero as well as non-zero H_{dc} , as described in Section III above, as well as the low-frequency noise data obtained in Ref. [36] on the same type of ceramics.

What could be the origin of that frustration? We believe that most probably it is the result of the d-wave nature of superconductivity in cuprates [15] and randomness of the crystalline orientations in ceramics [13, 14]. It was shown there that the form of the effective phase-dependent Hamiltonian for such ceramics is of the same form as in (I.1) except for the fact that the random phases α_{ij} at $B = 0$ are just 0 or π depending on the mutual orientation of grains i and j. Therefore such a system at $B = 0$ is equivalent to the XY spin glass, with the low-temperature state characterized by a completely

random orientation of phases ϕ_i, as in the gauge-glass model with uniformly random distribution of α_{ij}'s.

Therefore the low-temperature state is characterized by the presence of randomly distributed intergrain currents and, therefore, of the magnetic field generated by these currents. It means that the actual phases α_{ij} will contain contributions due to the self-induced magnetic field. Its relative importance is characterized by the ratio of the corresponding magnetic flux penetrating elementary loops of the ceramics Φ_{sf} to the flux quantum Φ_0, i.e. just by the parameter $\beta_L = 2\pi\mathcal{L}I_c/c\Phi_0$ where $\mathcal{L}$ is the characteristic inductance of an elementary loop [9]. Estimating the elementary inductance as $\mathcal{L} \approx 2\pi a_0\mu_g$ and using Eq.(IV.15) to estimate I_c, we obtain

$$\beta_L \approx \frac{4\pi^2 a_0\mu_g I_c}{c\Phi_0} = \frac{8\pi^3\mu_g a_0 E_J}{\Phi_0^2} \approx 0.1 \qquad \text{(IV.16)}$$

so the self-field (screening) effects are relatively weak, though perhaps not always negligible.

It is also of interest to estimate the effective penetration depth λ_{cer} of a very weak magnetic field perturbation δH into the ceramics. Roughly, the value of λ_{cer} can be estimated as $a_0/\sqrt{\beta_L} \sim 15\mu m$. Another (hopefully more accurate) estimate can be obtained using mean-field results [5] which allow one to express λ_{cer} via the critical current density J_c:

$$\lambda_{cer} = \left(\frac{\gamma}{8\pi^2}\frac{c\Phi_0}{J_c\xi_0\mu_g}\right)^{1/2} \approx 25\mu m \qquad \text{(IV.17)}$$

where we inserted (as compared with Ref. [5]) $\mu_g \approx 0.35$ and approximated the random nearest-neigbour network by a cubic lattice with coordination number $Z = 6$, which amounts to the relation $\xi_0^2 = a_0^2/6$ between the effective interaction range ξ_0 and the intergrain distance a_0.

The characteristic magnetic field variation producing the critical current density J_c at the boundary can be estimated as $\Delta H_c \sim 4\pi\lambda_{cer}J_c/c \approx 15mG$, whereas the numerical solution [5] gives

$$\Delta H_c = \frac{\upsilon}{2c\gamma}4\pi\lambda_{cer}J_c \approx 30mG \qquad \text{(IV.18)}$$

Within the theoretical approach of Ref. [5], ΔH_c marks a crossover between reversible (although still non-linear at $\Delta H \leq \Delta H_c$) and irreversible penetration of the magnetic field into the intergrain network. The value of ΔH_c obtained in Eq.(IV.18) is on the lower border of the range of the field variations used to measure our d.c. magnetization curves, so we could just conclude that we always have $\delta H \gg \Delta H_c$ and thus are producing the Bean-like critical state. Indeed, the data at $H_{dc} = 0$, $T = 10K$ look compatible with such an interpretation (cf. Fig.(14), where some deviations from the logarithmic slope 1 (which is the characteristic of a Bean state) are seen at lowest $\Delta H \leq 50mG$).

However, as far as the data obtained at $10\,K$ with d.c. fields $H_{dc} \simeq 2G$, or all data at higher temperature ($T = 20K$), including d.c. and a.c. results at zero-H_{dc}, are concerned (cf. Figs.(12-16)), the low-field magnetization response is drastically different from Bean-type predictions, as explained at the end of Section III. Qualitatively, the most surprising feature of these data is the existence of a very broad range of ΔH within which the response is non-linear but still not like the critical-state one. We are not aware of any microscopic theory which predicts fractional-power behaviour of the shielding susceptibility over such a broad range of ΔH variations. It cannot be excluded *a priori* that such a behaviour is related to a very wide range of intergrain critical currents, which might exist in ceramics (till now we have neglected inhomogenity of intergrain coupling strengths in our theoretical discussion). Moreover, we may expect that the relative importance of such inhomogenities increases with the field and/or temperature (cf. Ref. [40])

In Section V, we will try to formulate a new phenomenological model appropriate for the understanding of our data (leaving its theoretical justification for a future study); this model will be seen to be an interpolation between Campbell's and Bean's regimes of flux penetration into hard superconductors.

V Fractal model of diamagnetic response

We showed at the end of Section III-C that a simple generalization, Eq.(III.14), of Bean's relation between variation of the applied magnetic induction ΔB and current J results in reasonably good agreement with our data. However, contrary to the original Bean relation, the new one was not based on any physical picture; it was just a convenient description of the data. In this Section we propose a phenomenological model which provides a qualitative understanding of the irreversible diamagnetic behaviour mimicked by Eq.(III.14).

We start from the picture of non-linear response of the current $\mathbf{J}$ to a variation of the vector potential $\delta\mathbf{A}$ derived in Ref. [5] within the mean-field approximation and presented in Fig. 2 of that paper. Here the current induced by a variation of $\delta\mathbf{A}$ is linear at very small $\delta\mathbf{A}$, then grows sublinearly, and finally reaches its maximum value J_c at the critical δA_c such that the differential response $(dJ/dA)_{\delta A_c} \to 0$. At $\delta A > \delta A_c$ the numerical in-

stability of the *slow cooling* equations was detected and interpreted as an indication of the absence of any solution which would interpolate smoothly between zero and large (i.e. $\gg \delta A_c$) values of δA. In other terms, some kind of "phase slip" was expected to happen in the model [5], leading to a new metastable state, which would have lower (free) energy at the new value of the vector potential $\mathbf{A}' = \mathbf{A} + \delta\mathbf{A}$ (in other terms, a state similar to the one obtained by the F.C. procedure at constant $\mathbf{A}'$, which does not carry macroscopic current). Further increase of $\delta\mathbf{A}' = \mathbf{A} - \mathbf{A}'$ again induces a macroscopic current until it reaches the maximum value J_c at $\delta A' = \delta A_c$, and so on. Thus the whole $J(\delta A)$ dependence emerging from the mean-field solution [5] is periodic; it leads immediately to the irreversibility of the response, since the inverse function $\delta A(J)$ is multivalued: different vector potential values may correspond to the same value of current. Of course, such a periodic $J(\delta A)$ dependence does not correspond to the usual Campbell - Bean picture, which would better be represented by

$$J_{C.-B.}(\delta A) = J(\delta A)\theta(\delta A_c - \delta A) + J_c\theta(\delta A - \delta A_c) \quad \text{(V.19)}$$

It is important to note that the $J(\delta A)$ dependence Ref. [5] was obtained from the *space-independent* solution for the glassy correlation function $Q_{jj}(t,t') =< cos(\phi_j(t) - \phi_j(t')) >$; such an approximation, being reasonable for the description of smooth "adiabatic" transformations in a system with long-range interactions, will probably break down when the jump from one metastable state to another happens. In other terms, the above-mentioned "phase slip" should have something to do with spatially inhomogeneous processes like vortex penetration in hard type-II superconductors. The problem of the solution of the general history- and space-dependent system of integral equations (which may be derived following the method of Ref. [5]) is formidable and the method to solve it is still unknown. Therefore we can only speculate on possible properties of its solution. The simplest idea would be that the macroscopic $J(\delta A)$ response becomes (after averaging over inhomogenities of the space-dependent solution) similar to the Campbell-Bean type of the response (V.19). Indeed, our analysis of the low-field diamagnetic response at $T = 10K$ and $H_{ext} = 0$ (Section III-B) developed in Section IV on the basis of such an assumption, is in reasonable agreement with the data. However other sets of data (for higher temperature and/or lower field) are described by completely different *Ansatz* (III.13). We will now propose a (phenomenological) generalization of the $J(\delta A)$ relation compatible with Eq.(III.13). The relation we are looking for should be an *intrinsic* (i.e. independent on the sample geometry) and *general* (i.e. usable for an arbitrary magnetic history of the sample) relation between the current and variation of the vector potential. Remember that Eq. (III.13) was written for the simplest nonmonotonic variation of ΔB, and that it relates the true vector $\mathbf{J}$ and the pseudovector $\Delta\mathbf{B}$. So, in writing this equation, some additional information on the geometry of the sample has been used (we use the simplest slab geometry). Thus a natural basic equation should relate the current density $\mathbf{J}$ and the variation of the vector potential $\delta\mathbf{A}$.

In a generalized model, the diamagnetic current response should possess two major properties:
i) it must scale as some fractional power $\alpha \approx 0.5$ with the amplitude of exitation field δB, and
ii) it must be strongly irreversible (as it follows from the analysis of the ratio $4\pi\chi''/(1 - 4\pi\chi') \approx 0.28$). We consider these two conditions in sequence.

The condition i) is rather easy to fulfill: it is enough to suppose that the differential response of the current to the variation of the vector potential δA is given by a non-linear generalization of the London relation

$$\frac{d\mathbf{J}}{d\mathbf{A}} = -\frac{c}{4\pi}\lambda_{eff}^{-2}(J) \quad \text{(V.20)}$$

where the current-dependent "effective penetration depth" is given by

$$\lambda_{eff} = \lambda_1 |J/J_1|^{\kappa} . \quad \text{(V.21)}$$

In the case of a monotonic field variation applied to an initially uniform induction distribution, the Eqs.(V.20, V.21) lead to the simple relation $J \propto \Delta B^{\alpha}$ with $\alpha = (1+\kappa)^{-1}$. Indeed, with $dA = \Delta B\, dx$ and approximating $d\Delta B/dx$ by $\Delta B/\lambda_{eff}$, one obtains $J \propto \Delta B^{\frac{1}{1+\kappa}}$. Thus we need to choose $\kappa \approx 1$ in order to reproduce the observed scaling with $\alpha \approx 0.5$.

However, the set of equations (V.20, V.21) does not fulfill the second condition ii) above: the corresponding solutions are *reversible*, as it follows from the existence of a single-valued function $\delta A(J) \propto J^{1+2\kappa}$ which follows from Eqs.(V.20, V.21). In other words, the system described by Eqs.(V.20, V.21) would exhibit nonlinearity and harmonics generation, but would not show finite $\chi''(\omega)$ in the $\omega \to 0$ limit. In order to avoid this inconsistency, we need to formulate a model with the same kind of scaling between δA and J as in Eqs.(V.20, V.21), but with a nonmonotonic $J(\delta A)$ dependence allowing for the irreversible behaviour.

A model obeying very similar properties was formulated and studied in Ref. [41] in a different physical context (one-dimensional spin glass). The low-energy spin configurations in this model are described by a phase variable $\varphi(x) \in (-\pi, \pi)$ such that two such configurations (local energy minima) which differ by a phase shift

$\delta\varphi(x_0) = \Phi$ in a region around some point x_0, have a characteristic energy difference $E(\Phi) \propto \Phi^{5/3}$ and a characteristic spatial extent of the phase deformation $X(\Phi) \propto \Phi^{1/3}$. This scaling holds for the intermediate range of phase deformations $\varphi_0 \ll \Phi \ll \pi$; at smaller $\Phi \leq \varphi_0 \ll 1$ the energy cost of deformation is $\propto \Phi^2$, whereas at $\Phi \sim \pi$ the energy growth obviously saturates due to 2π periodicity. The above $E(\Phi)$ scaling leads to a *sublinear growth* of the characteristic "force" $f(\Phi) = dE/d\Phi \propto \Phi^{2/3}$ with Φ in the same intermediate range. The main contribution to the second derivative $d^2E/d\Phi^2$ (curvature of the energy valleys) comes from the smallest scale $\Phi \sim \varphi_0$, i.e. from the curvature of individual local minima. It was explained in Ref. [41] that such a scaling means a fractal organization of the energy minima as a function of φ with fractal dimensionality $D_f = 1/3$. It means that the number of energy minima discernable on a scale φ grows as $\mathcal{N} \propto \varphi^{-1/3}$ at finer scales; new minima appear primarily due to the splitting the older (broader) ones. This picture emerged in Ref. [41] from the microscopic analysis of the original Hamiltonian for a one-dimensional spin-glass model formulated in Ref. [42]. We can borrow the qualitative features of this construction for our present purpose (leaving for future studies the problem of its microscopic justification for the case of superconductive glasses).

Suppose that the free energy $F(\delta A)$ of the Josephson network behaves (as a function of vector potential variations with respect to a "virgin" state with a homogeneous induction) in a way similar to $E(\varphi)$ at $\varphi \ll \pi$. Namely, suppose that the free energy is parabolic, $\delta F \propto (\delta A)^2$, at very small variations of vector potential $\delta A \leq \delta A_{c1}$, but on a larger scale, $\delta A \gg \delta A_{c1}$, it contains many local minima whose characteristic free energies scale (with respect to the lowest state with $\delta A = 0$) as

$$F(\delta A) \propto (\delta A)^{\theta+1} \, for \delta A_{c1} \ll \delta A \ll \delta A_c \qquad \text{(V.22)}$$

with the exponent $\theta \in (0,1)$ (see the definition of δA_c below). Then the characteristic value of the current $J = \frac{1}{c}\partial F/\partial A$ scales as

$$J_{char}(\delta A) \approx J_{c1}\left(\frac{\delta A}{\delta A_{c1}}\right)^{\theta} \qquad \text{(V.23)}$$

in the same interval of δA. At large $\delta A \geq \delta A_c$ variations, the growth of the induced current should saturate at the true critical current value J_c, so we can estimate

$$\delta A_c \sim \delta A_{c1}(J_c/J_{c1})^{1/\theta}. \qquad \text{(V.24)}$$

On the other hand, weak $\delta A \ll \delta A_{c1}$ leads to the usual linear London (or Campbell) response with an effective penetration depth λ_1; matching at $\delta A \sim \delta A_{c1}$ leads to the following estimate:

$$\delta A_{c1} \sim \frac{4\pi}{c} J_{c1}\lambda_1^2 \qquad \text{(V.25)}$$

The estimate (V.23) looks very much like the previous version defined by (V.20, V.21), so one can find the relation between the exponents:

$$\theta = 1/(1+2\kappa) = \alpha/(2-\alpha) \approx 0.3 \qquad \text{(V.26)}$$

Figure 18: Picture of a fractal $J(\delta A)$ landscape. An example of a hysteresis loop is shown.

However the whole picture is substantially altered: the current is now supposed to be an (irregularly) oscillating function of δA (see Fig. 18), thus only its envelope $J_{char}(\delta A)$ defined on a scale δA follows the scaling relation (V.23). As a result, the inverse function $\delta A(J)$ is multivalued and the irreversibility of the response is ensured. Similar to the spin-glass model of Ref. [41], the fractal dimensionality D_f of the low-energy valleys can be defined; it is given now by $D_f = 1 - \theta \approx 0.7$. The proposed picture is based on the existence of two substantially different scales of currents, J_{c1} and J_c, and corresponding vector potential variations δA_{c1} and δA_c; thus it can be compared with the usual Campbell-Bean picture of critical currents in the same way as the thermodynamics of type-II superconductors is compared with that of the type-I ones.

In order to describe quantitatively the diamagnetic response in the "fractal" range (V.22) we need to determine the *distribution function* $\mathcal{P}[J(\delta A)]$ (which would lead, in particular, to the estimate (V.23) for $J_{char}(\delta A)$). Moreover, in general, a relation of the type of (V.23) could be

nonlocal (i.e. the current depends on the $\delta A(x)$ distribution in some region of space, whose size may depend on δA itself (see again Ref. [41]). We leave this complicated problem for future studies, and just note here that merely the existence of relation (V.23) is sufficient for the existence of some "natural" properties of the response (like the presence of a closed hysteresis loop, as it was assumed in Section III-C).

VI Summary and conclusions

In this paper, we have presented experimental results on the low temperature ($10\,K$ and $20\,K$) response of the granular HT_c superconductor $La_{1.8}Sr_{0.2}CuO_4$ to small field excitations. The general properties of the magnetic response were investigated in two samples (A and B) differing by the strength of the coupling between grains. By cooling the samples in various d.c. fields up to $20\,G$ and applying small field increases, we were able to measure the shielding response of the material and to derive a method, inspired by the work of Dersh and Blatter [22], to extract from the data the polarizability of the intergrain currents system. The field cooled (F.C.) magnetization was measured in fields up to $20\,G$. Analysis of the results led to the conclusion that i) the structure of the grains is polycrystalline, resulting in a step decrease of the F.C. magnetization with increasing field, which can be interpreted on the basis of the model by Wohllebeen et al. [29]; ii) self shielding (pinning) by the intergrain currents when lowering the temperature strongly reduces the value of the F.C. magnetization; iii) there is no macroscopic Meissner magnetization due to the system of intergrain currents.

Further detailed study of the response of the Josephson network was performed in sample B. It was shown that the response is asymmetric with respect to the sign of variation of the applied field after field cooling; this is due to the shielding currents pinned during cooling. The macroscopic critical current is found to be strongly reduced by moderate values of the external d.c. field, about $2\,G$.

Very low field magnetization measurements were performed by applying field steps of $10\,mG$ or low frequency a.c. fields in the range $50\,\mu G$ to $30\,mG$, after cooling in d.c. fields up to $8.8\,G$. The results show that the response is strongly non linear, the shielding current growing *sublinearly* with increasing applied field. Furthermore, the a.c. results show that it is strongly *irreversible* down to the smallest excitations used. It is shown that a non-linear relation between the shielding current and the induction, $J \propto \Delta B^{\alpha}$ with $\alpha \approx 0.5$, together with a natural assumption about the existence of a closed hysteresis loop, give predictions in a reasonable agreement with the data.

Theoretical analysis of our experimental results was developed on the frame of the existing "gauge-glass" theories. It was show that the extremely low value of the low-temperature, zero-field critical current density ($J_c \approx 3.7\,A/cm^2$ at $10\,K$) together with the rather high temperature of the transition to the low-temperature glassy state, can be coherently interpreted only under the assumption that the Josephson network is strongly frustrated even at zero applied field. This contradicts the usual assumption that frustration in the interactions arises only due to the local magnetic induction, but supports the hypothesis of the existence of a large proportiont of π-junctions in the granular system. These π-junctions are possibly due to the d-wave nature of the pairing, combined with the randomness of grain orientations in $La_{1.8}Sr_{0.2}CuO_4$ ceramics.

Finally, a new model of diamagnetic response in the glassy state of granular superconductors was developed in order to describe the anomalous (fractional-power) behavior of the shielding current response. This model, based on the idea of a fractal organization of the free energy landscape in the granular network, can provide a qualitative account for the main features of the anomalous response. Its further development will be the subject of future studies.

VII Acknowledgements

We are grateful to L. B. Ioffe for many important discussions which helped to clarify a number of issues considered in this paper. Research of M.V.F. was supported by the DGA grant # 94-1189, by the joint grant M6M300 from the International Science Foundation and the Russian Goverment, and by the grant # 95-02-05720 from the Russian Foundation for Fundamental Research.

A Appendix

The hysteretic behavior of the current as a function of the induction variations is represented by the relation:

$$\Delta J = \pm 2^{(1-\alpha)\nu} J_c \left(\frac{|\Delta B|}{B_c} \right)^{\alpha} \qquad \text{(A.27)}$$

$\nu = 0$ when starting from zero induction state, and 1 otherwise. $\Delta J = J - J_o$ and $\Delta B = B - B_o$ where J_o and B_o are the (old) values just before the last reversal of the sign of variation of B. The *Ansatz* A.27 ensures that we

have a stable closed hysteresis loop, and that there is no hysteresis for $\alpha = 1$ which describes the London case. Figure 19 displays the shape of the hysteresis loops for three characteristic values of α. The induction profile is

Figure 19: Hysteretic behavior of the current for a variation of the induction between $-B_c$ and B_c.

determined by the Maxwell equation which leads, for the case of weak penetration, to

$$\frac{d\Delta B}{dx} = \pm 2^{(1-\alpha)\nu}\mathcal{A}\,|\Delta B|^{\alpha} \qquad \text{(A.28)}$$

where $\mathcal{A} = 4\pi J_c/B_c^{\alpha}$; x is the distance from the edge of the sample. After increasing applied field from 0 to h_o, starting from zero induction state, the induction profile is given by $B^{-\alpha}dB = -\mathcal{A}\,dx$, leading to:

$$x = -\frac{1}{\mathcal{A}}\int_{h_o}^{B}\xi^{-\alpha}d\xi = -\frac{B^{1-\alpha} - h_o^{1-\alpha}}{(1-\alpha)\mathcal{A}}$$

where

$$B = \left(h_o^{1-\alpha} - (1-\alpha)\mathcal{A}\,x\right)^{\frac{1}{1-\alpha}}. \qquad \text{(A.29)}$$

Field penetrates till $x = x_{h_o} = h_o^{1-\alpha}/(1-\alpha)\mathcal{A}$.

When h decreases from h_o, we get $(B_o - B)^{-\alpha}dB = -2^{1-\alpha}dx$. Hence:

$$x = -\frac{1}{2^{1-\alpha}\mathcal{A}}\int_{h_o-h}^{B_o-B}\xi^{-\alpha}d\xi$$

$$= -\frac{1}{2^{1-\alpha}\mathcal{A}(1-\alpha)}\left((B_o - B)^{1-\alpha} - (h_o - h)^{1-\alpha}\right)$$

Modification of induction relative to B_o extends up to $x_h = (h_o - h)^{1-\alpha}/2^{1-\alpha}\mathcal{A}$. For $0 < x < x_h$,

$$B = B_o - 2\left(\left(\frac{h_o - h}{2}\right)^{1-\alpha} - (1-\alpha)\mathcal{A}\,x\right)^{\frac{1}{1-\alpha}} \qquad \text{(A.30)}$$

Figure 20: Induction profile as a function of applied field. R_o is the maximum abcissa of field penetration.

where B_o is given by Eq. (A.29). When $h = -h_o$ is reached, Eq. (A.30) gives simply $B = -B_o$. After reversing the sign of variation of h once more, the profiles are simply symmetrical of those given by Eq. (A.30). Examples of induction profiles are given on Fig. 20 for $\alpha = 0.5$. The average induction can be derived now. After some algebra, one obtains:

$$< B >= \frac{\mathcal{A}}{2-\alpha} \times h_o^{2-\alpha}\left[1 - 2\left(\frac{1 - h/h_o}{2}\right)^{2-\alpha}\right]$$

for $h_o > 0$, and

$$< B >= \frac{}{2-\alpha} \times h_o^{2-\alpha}\left[-1 + 2\left(\frac{1 + h/h_o}{2}\right)^{2-\alpha}\right] \qquad \text{(A.31)}$$

for $h_o < 0$.

For a sinusoidal excitation $h = h_o\cos\omega t$, one gets

$$\frac{< B >}{h_o} = \frac{\mathcal{A}\,h_o^{1-\alpha}}{2-\alpha}\left[1 - 2\left(\frac{1 - \cos\omega t}{2}\right)^{2-\alpha}\right]$$

for $2n\pi < \omega t < (2n+1)\pi$

$$\frac{< B >}{h_o} = \frac{\mathcal{A}\,h_o^{1-\alpha}}{2-\alpha}\left[-1 + 2\left(\frac{1 + \cos\omega t}{2}\right)^{2-\alpha}\right] \qquad \text{(A.32)}$$

for $(2n-1)\pi < \omega t < 2n\pi$.

Since $< B > /h_o = 1 + < M > /h_o$, Fourier transformation gives the values of $1 + 4\pi\chi'$ and $4\pi\chi''$. This can be done numerically. Figure 21 displays the ratio $4\pi\chi''/1 + 4\pi\chi'$ as a function of α.

Figure 21: Values of $4\pi\chi''/1+4\pi\chi'$ as a function of α.

References

[1] For a review, see G. Blatter, M. V. Feigel'man, V. B. Geshkenbein, A. I. Larkin and V. M. Vinokur, Rev. Mod. Phys. **66**, 1125 (1994)

[2] S. John and T. C. Lubensky, Phys. Rev. **B34**, 4815 (1986).

[3] V. M. Vinokur, L. B. Ioffe, A. I. Larkin and M. V. Feigel'man, Sov. Phys. JETP **6**, 1986 (1987).

[4] V. S. Dotsenko, M. V. Feigel'man and L.B. Ioffe in Spin Glasses and Related Problems, Soviet Scientific Review /Section A, Chapter IV.

[5] M. V. Feigel'man and L. B. Ioffe, Phys. Rev. Lett. **74**, 3447 (1995).

[6] J. D. Reger, T. A. Tokuyasu, A. P. Young and M. P. A. Fisher Phys.Rev. **B44**, 7147 (1991).

[7] D. Huse and H. Seung, Phys.Rev. B 42, 1059 (1990).

[8] H. S. Bokil and A. P. Young Phys. Rev. Lett. **74**, 3021 (1995).

[9] M. Borik, M. Chernikov, V. Velasago and V. Stepankin, J. Low Temp. Phys. **85**, 283 (1991).

[10] D. S. Fisher, M. P. A. Fisher and D. A. Huse, Phys. Rev. **B43**, 130 (1991).

[11] E. B. Sonin, JETP Lett. **47**, 496 (1988); E. B. Sonin and A. K. Tagancev, Sov.Phys.JETP **68**, 572 (1989).

[12] B. Z. Spivak and A. Yu. Zyuzin JETP Lett. **47**, 267 (1988); B. Z. Spivak and S. Kivelson Phys. Rev. **B43**, 3740 (1991).

[13] V. B. Geshkenbein, A. I. Larkin and A. Barone, Phys. Rev. **B36**, 235 (1987).

[14] M. Sigrist and T. M. Rice, Reviews of Modern Physics **67**, 503 (1995).

[15] J. R. Kirtley, C. C. Tsuei, J. Z. Sun, C. C. Chi, L. S. Yu-Jahnes, A. Gupta, M. Rupp and M. B. Ketchen, Nature **373**, 225 (1995).

[16] H. Kawamura, Phys. Rev. **B51**, 12398 (1995) and J. Phys. Soc. Japan **64**, 711 (1995).

[17] I. Morgenstern, K. A. Müller and J. G. Bednorz, Z. Phys. **B69**, 33 (1987).

[18] P. Imbert and G. Jehanno, Hyperfine Interactions **47–48**, 233 (1989).

[19] C. P. Bean, Rev. Mod. Phys. **36**, 31 (1964).

[20] A. M. Campbell, J.Phys. **C2**, 3186 (1969).

[21] M. Ocio, M. Alba and J. Hammann, J. Physique Lett. **46**, 1101 (1985).

[22] H. Dersh and G. Blatter, Phys. Rev. **B38**,11391 (1988).

[23] J. A. Osborn, Phys. Rev. **67**, 351 (1945).

[24] U. Yaron, Y. Kornyushin and I. Felner, Phys. Rev. **B46**, 14823 (1992).

[25] C. P. Poole, T. Datte and H. A. Farach, Copper Oxide Superconductors, John Wiley & Sons, New-York 1988.

[26] R. Renker, I. Apfelstedt, H. Küpfer, C. Politis, H. Rietschel, W. Shauer, W. Wüll, U. Gottwick, H. Kneissel, U. Rauchschwalbe, H. Spille and F. Steglich, Z. Phys. **B67**, 1 (1987).

[27] The susceptibility, which in the usual sense is a local quantity representing $(B-H)/H$, has no meaning in the case of circulating currents in a conductor. We speak rather of a polarizability χ_j which represents the average value $< B-H > /H$, and describes the global effect of the currents over the whole volume of the sample.

[28] S. Ruppel, G. Michels, H. Geus, J. Kalenborn, W. Schlabitz, B. Roden and D. Wohllebeen, Physica **C174**, 233 (1991).

[29] D. Wohllebeen, G. Michels and S. Ruppel, Physica **C174**, 242 (1991).

[30] C. Ebner and D. Stroud, Phys. Rev **B31**, 165 (1985).

[31] T. Shibauchi, H. Kitano, K. Uchinokura, A. Maeda, T. Kimura and K. Kishio, Phys. Rev. Lett. **72**, 2263 (1994).

[32] M. Suzuki, Physica **C185–189**, 2243 (1991).

[33] Y. B. Kim, C. F. Hempstead and A. R. Strnad, Phys. Rev. Lett. **9**, 306 (1962).

[34] S. Senoussi, M. Ousséna, G. Collin and I. A. Campbell, Phys. Rev. **B37**, 9772 (1988).

[35] J. R. Clem, Physica **C153–155**, 50 (1988).

[36] L. Leylekian, M. Ocio and J. Hammann, Physica **B194–196**, 1865 (1994).

[37] L. Leylekian,M. Ocio and J. Hammann, Physica **C185–189**, 2243 (1991).

[38] L. B. Ioffe, Phys.Rev. **B38**, 5181 (1988).

[39] see the review Ref.[4], p.183.

[40] L. Glazman, A. Koshelev and A. Lebed', ZhETF **94**, 259 (1988); Sov.Phys.JETP **67**, 1235 (1988).

[41] see the review Ref.[4], Section 3.2.

[42] M. V. Feigel'man and L. B. Ioffe, Z.Phys.**B 51**, 237 (1983).

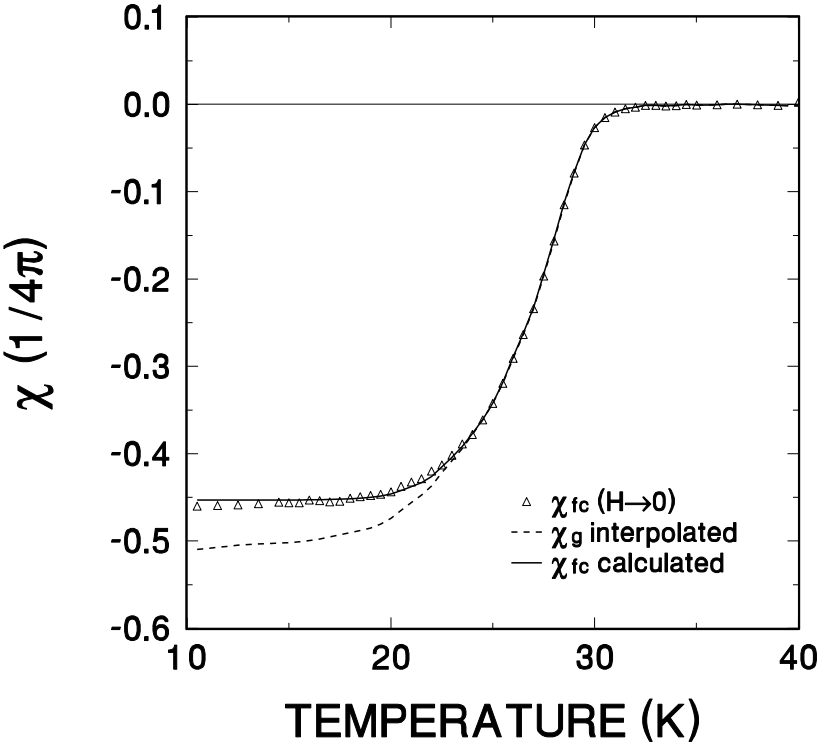
0.1
0.0
-0.1
-0.2
-0.3
-0.4
-0.5
-0.6
χ (1/4π)
10
20
30
40
TEMPERATURE (K)
χfc (H→0)
χg interpolated
χfc calculated

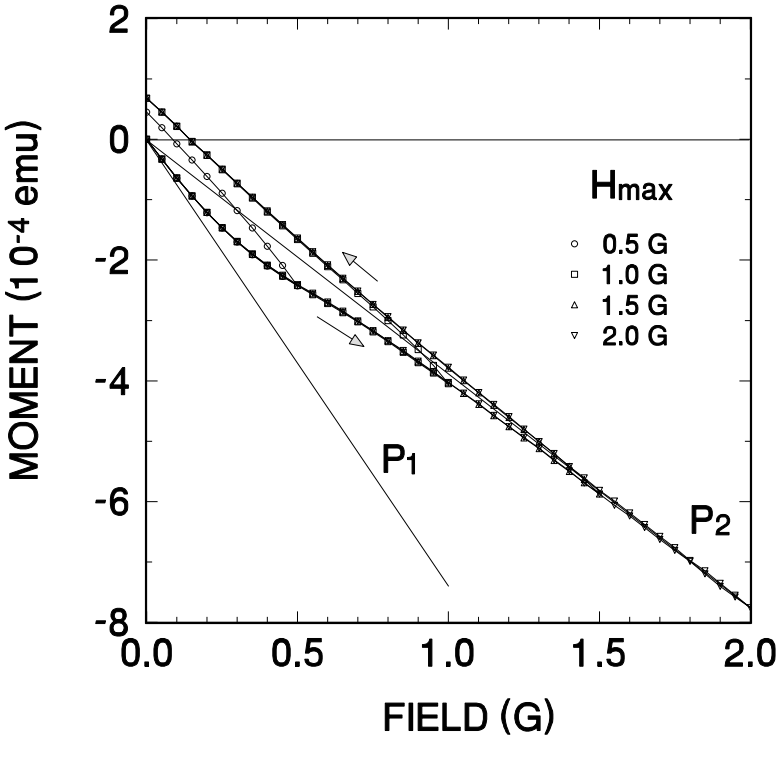
2
0
-2
-4
-6
-8
0.0
0.5
1.0
1.5
2.0
MOMENT (10-4 emu)
FIELD (G)
Hmax
0.5 G
1.0 G
1.5 G
2.0 G
P1
P2

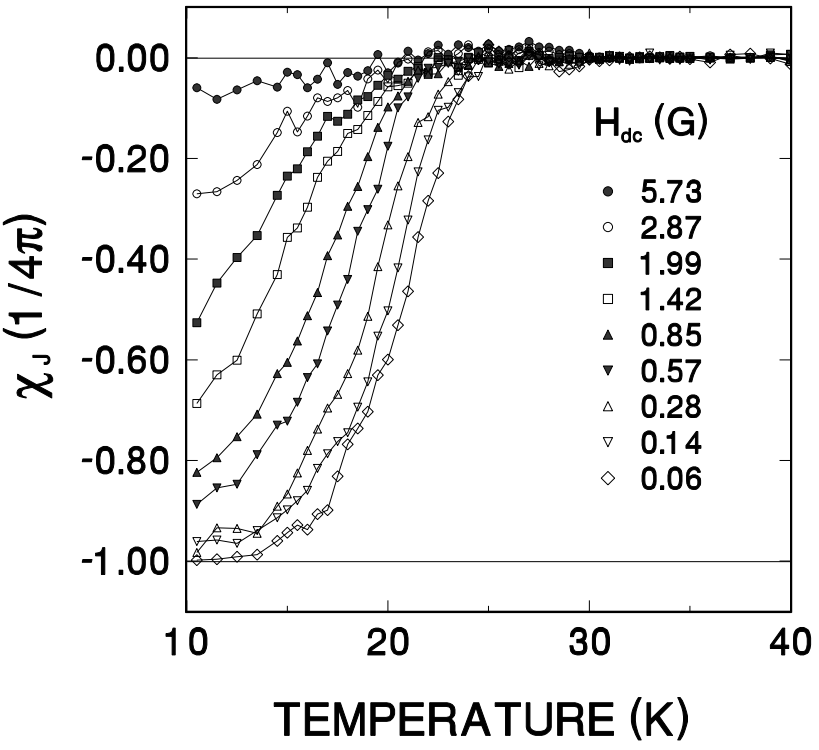
0.00
-0.20
-0.40
-0.60
-0.80
-1.00
χJ (1 /4π)
10
20
30
40
TEMPERATURE (K)
Hdc (G)
5.73
2.87
1.99
1.42
0.85
0.57
0.28
0.14
0.06

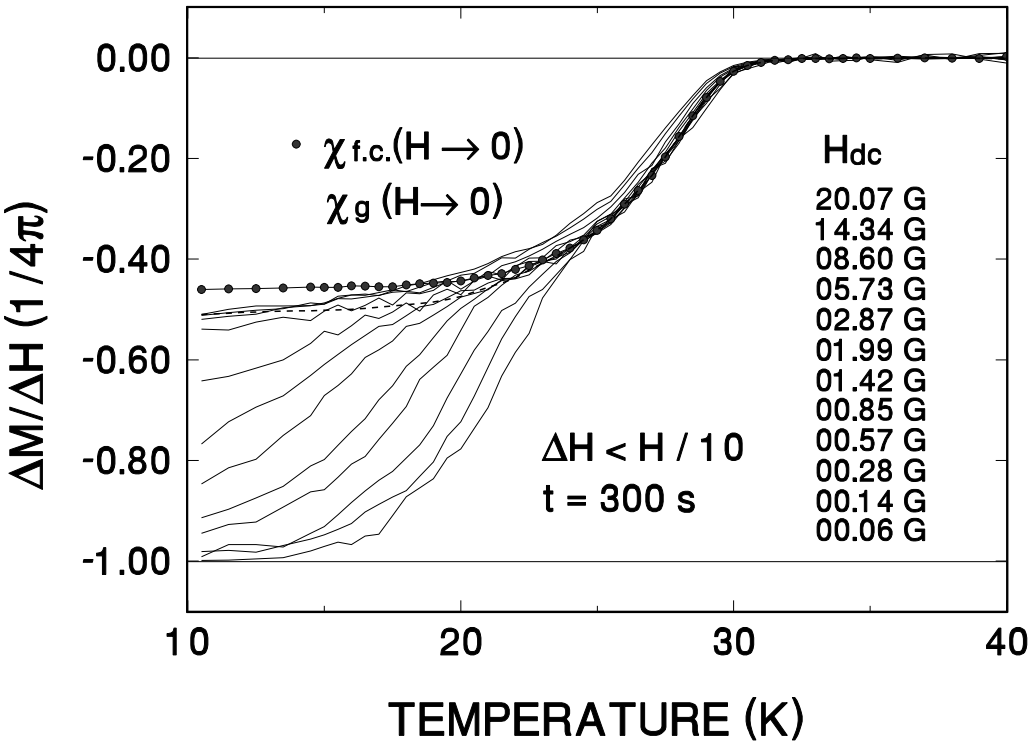
0.00
-0.20
-0.40
-0.60
-0.80
-1.00
ΔM/ΔH (1 /4π)
10
20
30
40
TEMPERATURE (K)
χ f.c.(H → 0)
χ g (H→ 0)
ΔH < H / 10
t = 300 s
Hdc
20.07 G
14.34 G
08.60 G
05.73 G
02.87 G
01.99 G
01.42 G
00.85 G
00.57 G
00.28 G
00.14 G
00.06 G

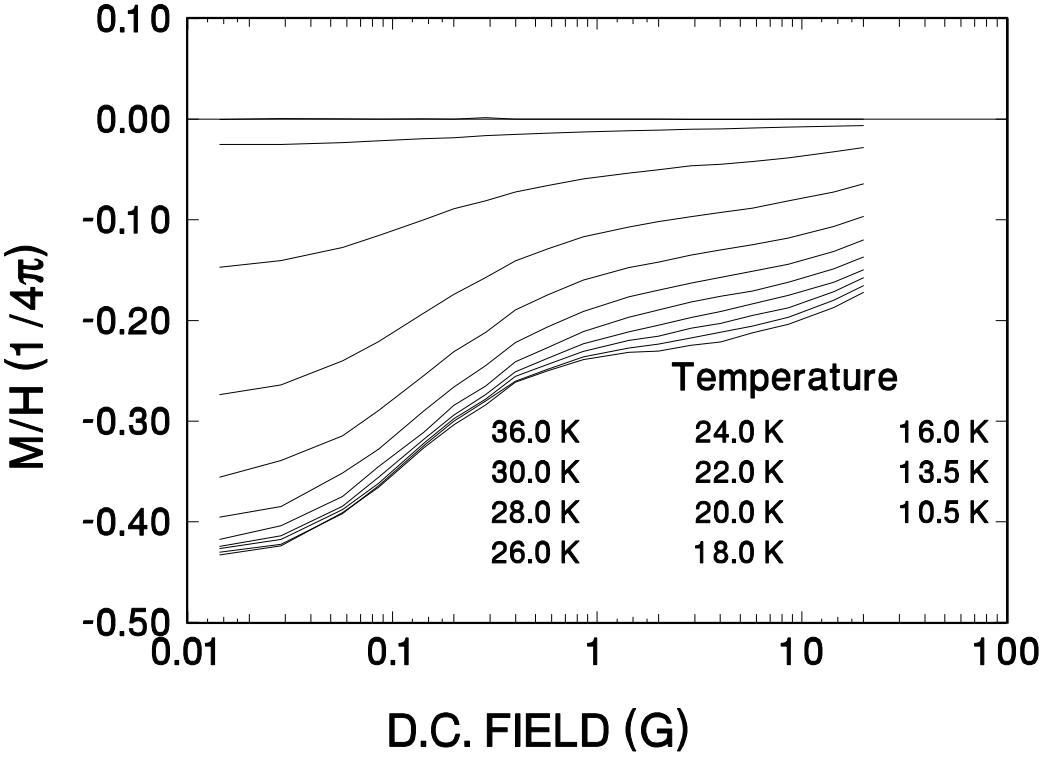
0.10
0.00
-0.10
-0.20
-0.30
-0.40
-0.50
M/H (1/4π)
0.01
0.1
1
10
100
D.C. FIELD (G)
Temperature
36.0 K
30.0 K
28.0 K
26.0 K
24.0 K
22.0 K
20.0 K
18.0 K
16.0 K
13.5 K
10.5 K

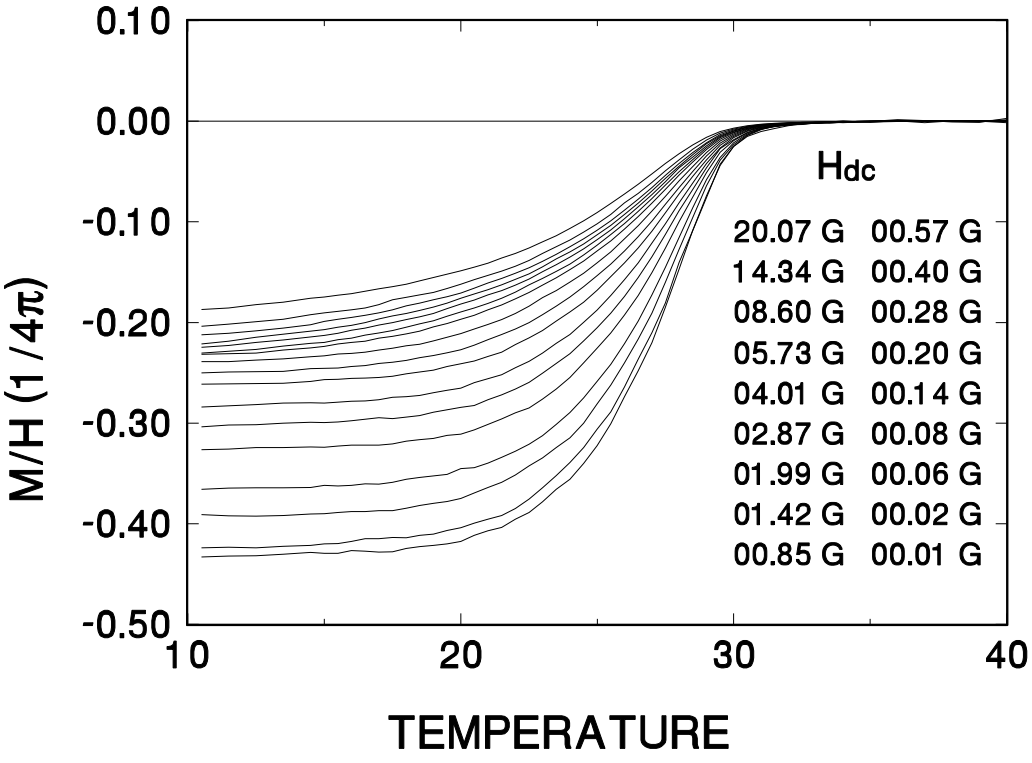
0.10
0.00
-0.10
-0.20
-0.30
-0.40
-0.50
M/H (1 /4π)
10
20
30
40
TEMPERATURE
Hdc
20.07 G 00.57 G
14.34 G 00.40 G
08.60 G 00.28 G
05.73 G 00.20 G
04.01 G 00.14 G
02.87 G 00.08 G
01.99 G 00.06 G
01.42 G 00.02 G
00.85 G 00.01 G

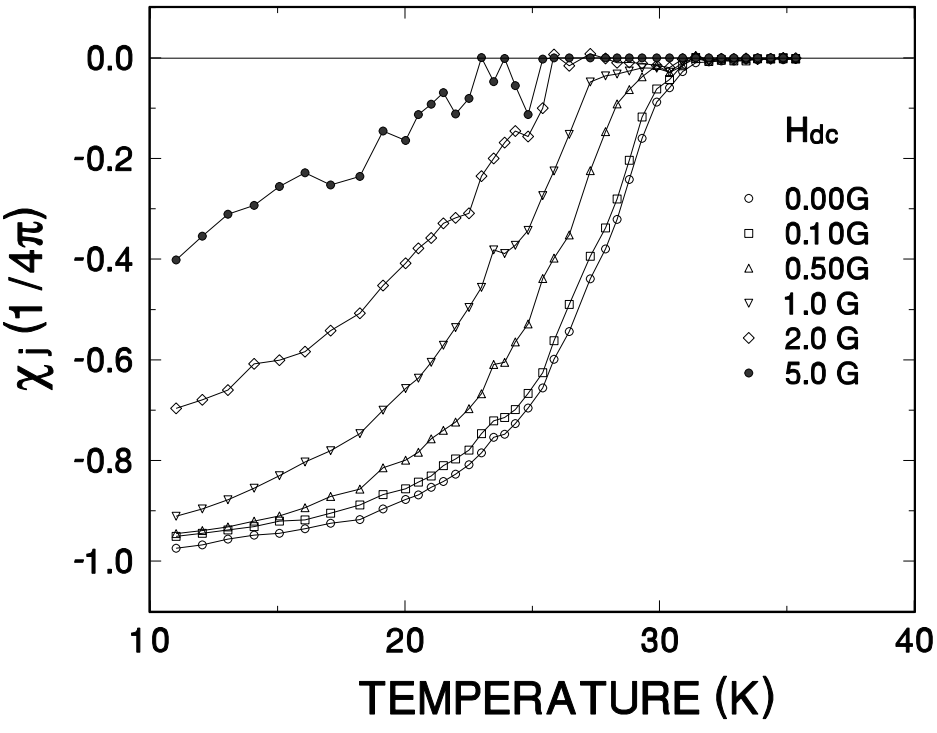
0.0
-0.2
-0.4
-0.6
-0.8
-1.0
χj (1/4π)
10
20
30
40
TEMPERATURE (K)
Hdc
0.00G
0.10G
0.50G
1.0 G
2.0 G
5.0 G

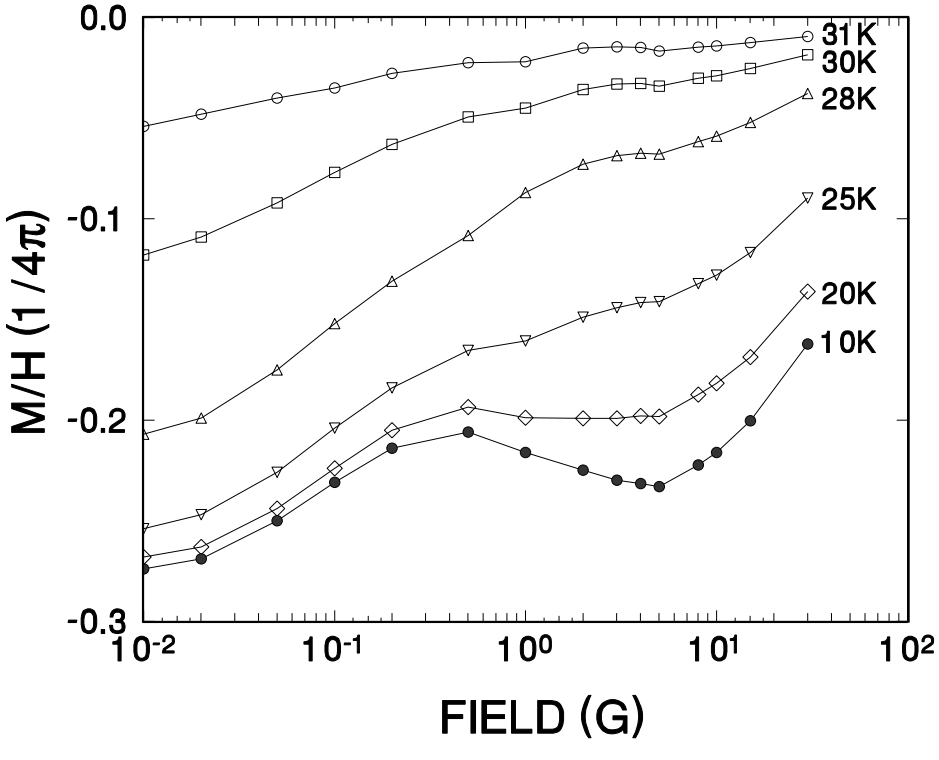
0.0
-0.1
-0.2
-0.3
M/H (1 /4π)
10-2
10-1
100
101
102
FIELD (G)
31K
30K
28K
25K
20K
10K

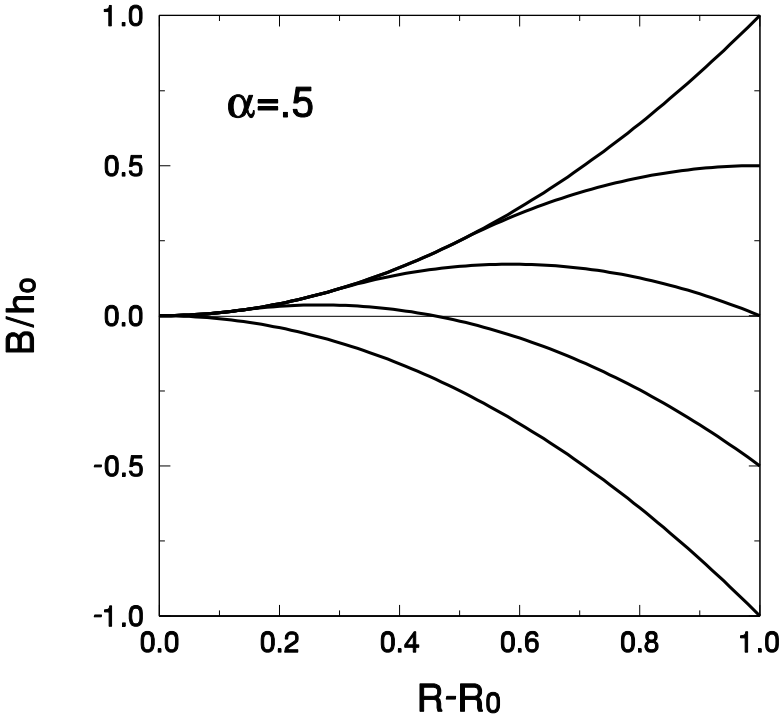
α=.5
1.0
0.5
0.0
-0.5
-1.0
B/h0
0.0
0.2
0.4
0.6
0.8
1.0
R-R0

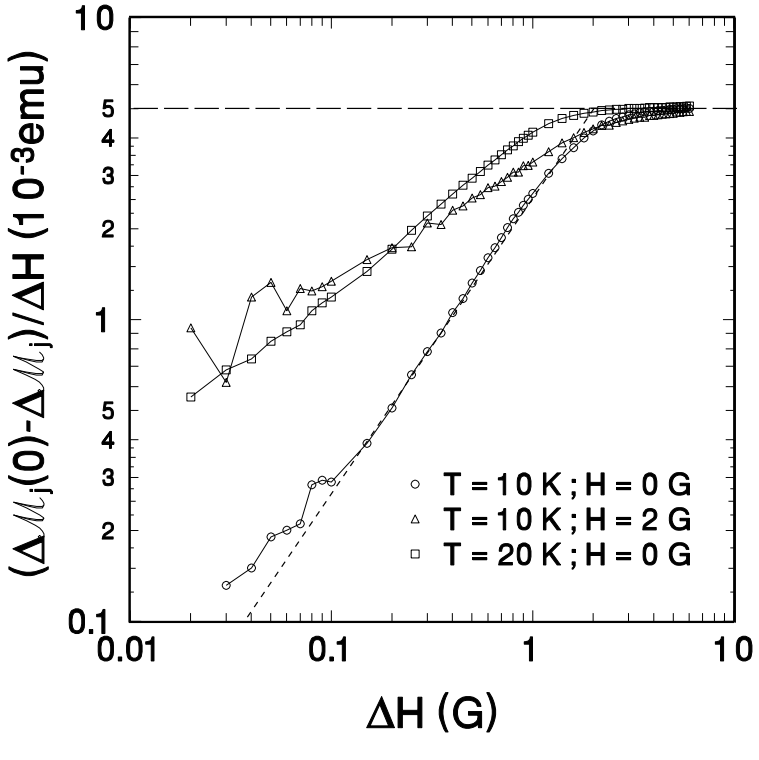
10
5
4
3
2
1
5
4
3
2
0.1
0.01
0.1
1
10
$(\Delta\mathcal{M}_j(0)-\Delta\mathcal{M}_j)/\Delta H$ (10^{-3}emu)
ΔH (G)
T = 10 K ; H = 0 G
T = 10 K ; H = 2 G
T = 20 K ; H = 0 G

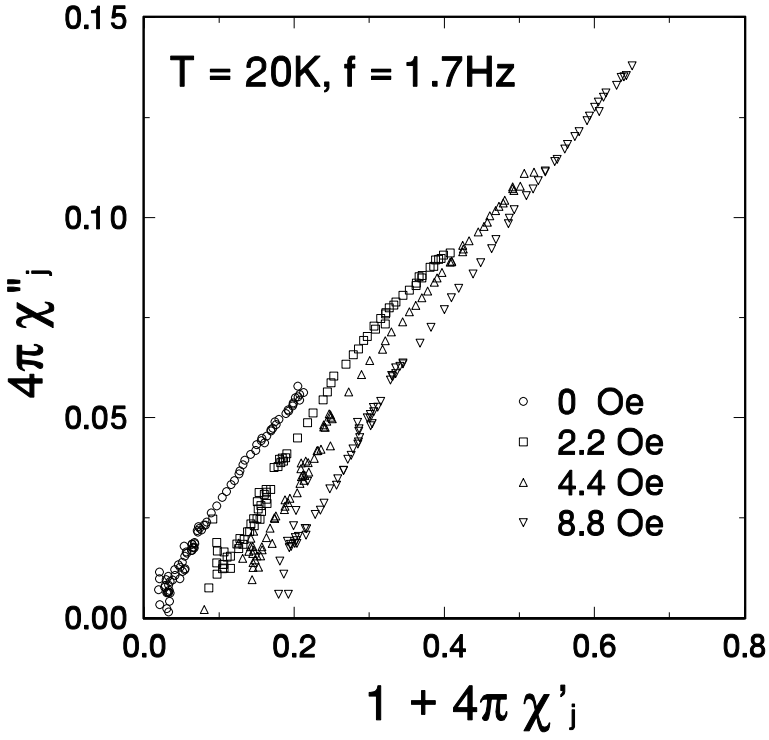
T = 20K, f = 1.7Hz
0 Oe
2.2 Oe
4.4 Oe
8.8 Oe
0.15
0.10
0.05
0.00
0.0
0.2
0.4
0.6
0.8
4π χ"j
1 + 4π χ'j

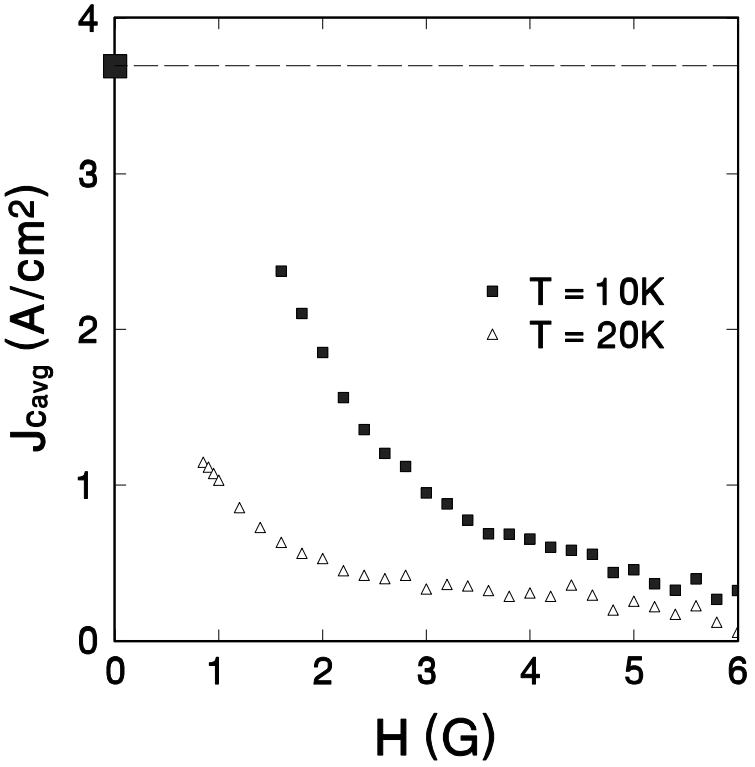
4
3
2
1
0
0
1
2
3
4
5
6
Jcavg (A/cm2)
H (G)
T = 10K
T = 20K

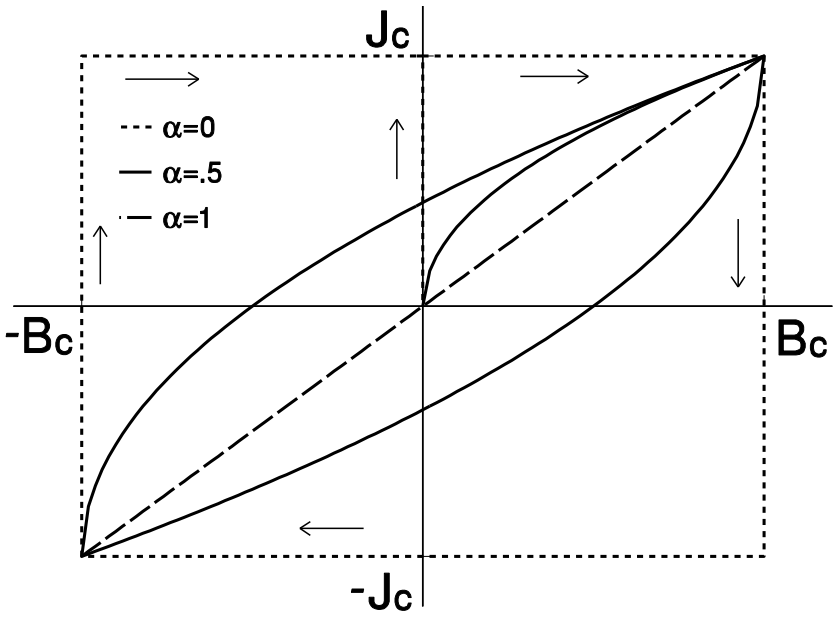
Jc
α=0
α=.5
α=1
-Bc
Bc
-Jc

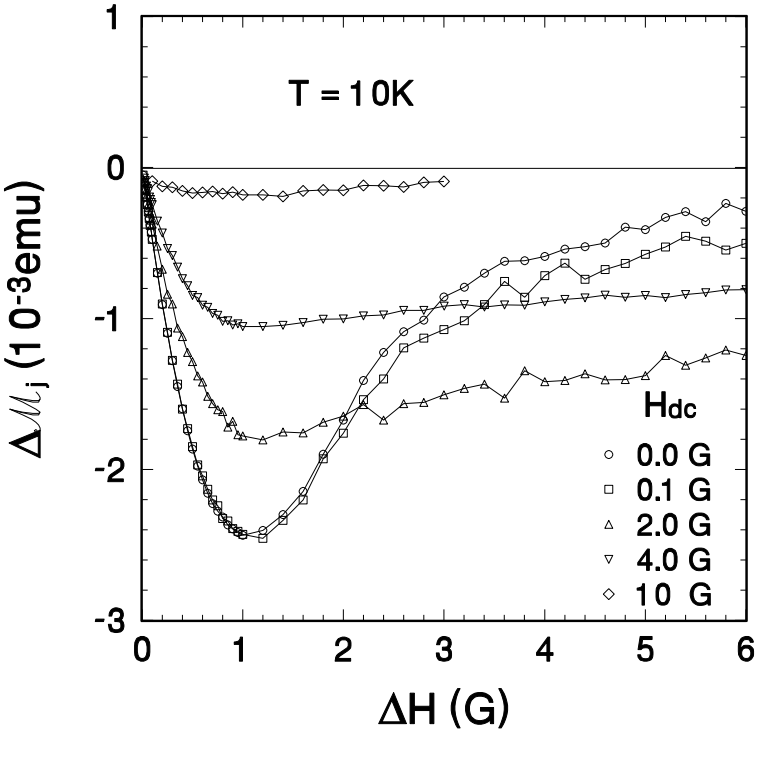
T = 10K
ΔM_j (10^{-3}emu)
ΔH (G)
H_{dc}
0.0 G
0.1 G
2.0 G
4.0 G
10 G
1
0
-1
-2
-3
0
1
2
3
4
5
6

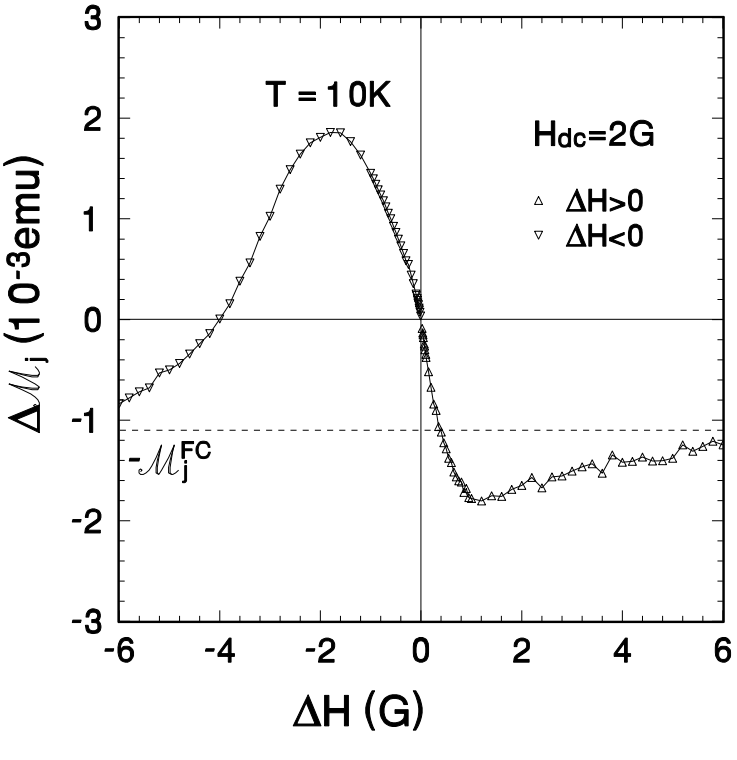
T = 10K
Hdc=2G
ΔH>0
ΔH<0
-$\mathcal{M}_j^{FC}$
$\Delta\mathcal{M}_j$ (10^{-3}emu)
ΔH (G)
3
2
1
0
-1
-2
-3
-6
-4
-2
0
2
4
6

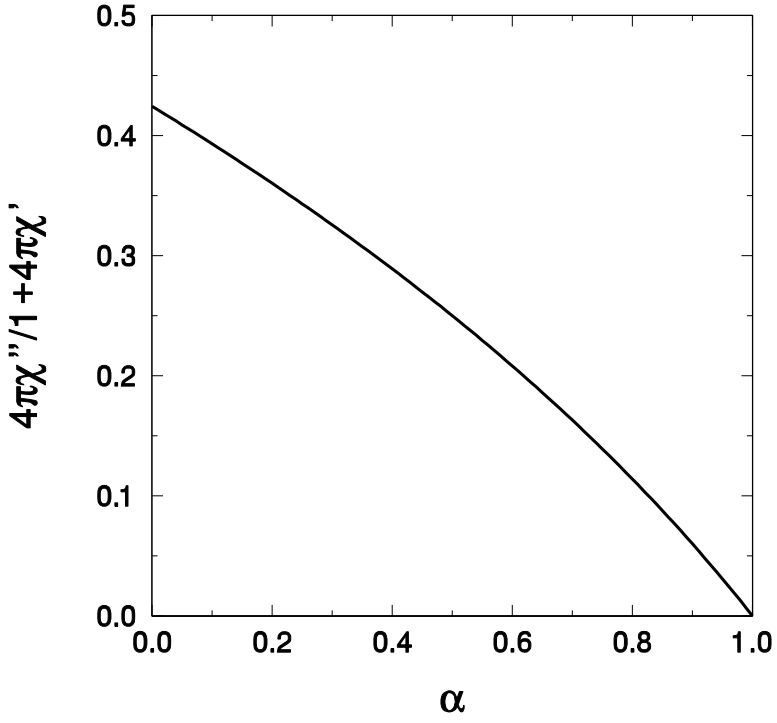
0.5
0.4
0.3
0.2
0.1
0.0
0.0
0.2
0.4
0.6
0.8
1.0
4πχ''/1+4πχ'
α

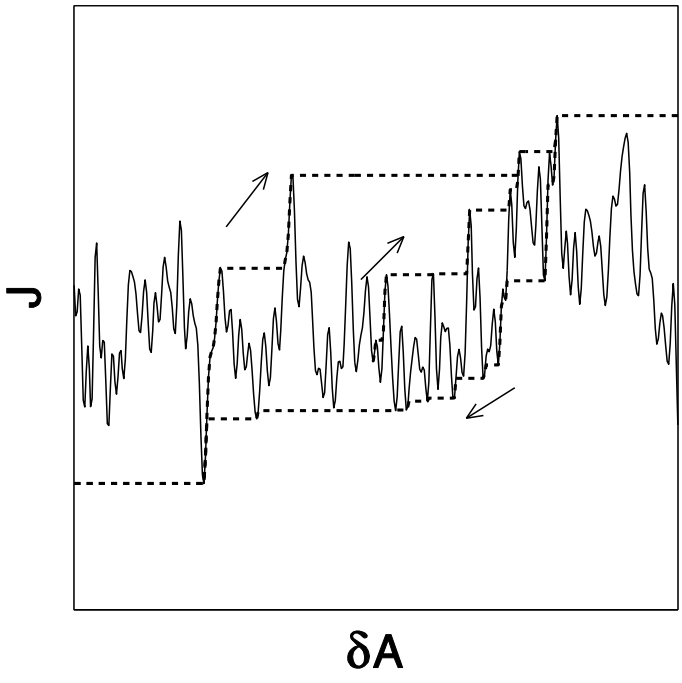
J
δA

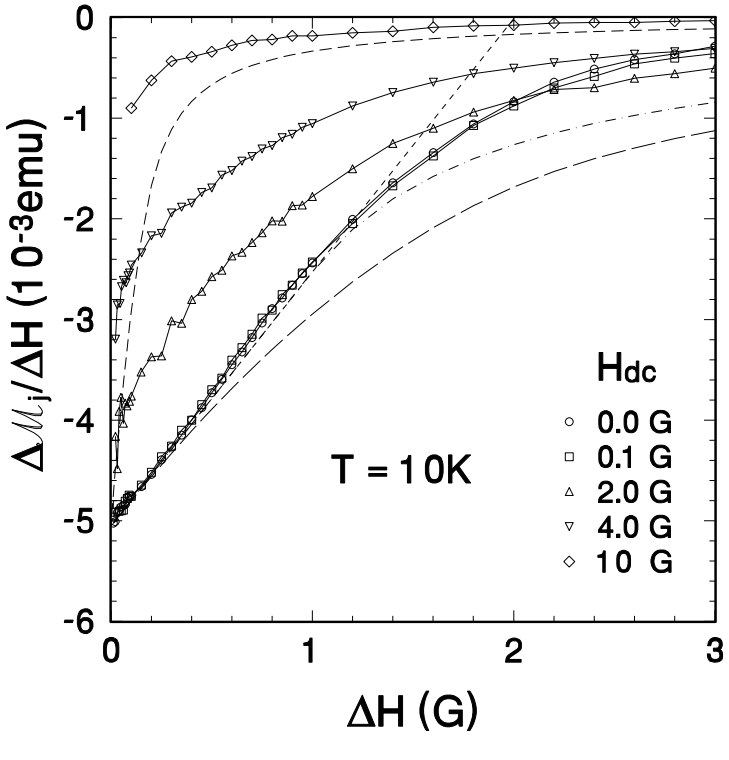
0
-1
-2
-3
-4
-5
-6
0
1
2
3
ΔH (G)
Δ𝓜ᵢ/ΔH (10⁻³emu)
T = 10K
Hdc
0.0 G
0.1 G
2.0 G
4.0 G
10 G

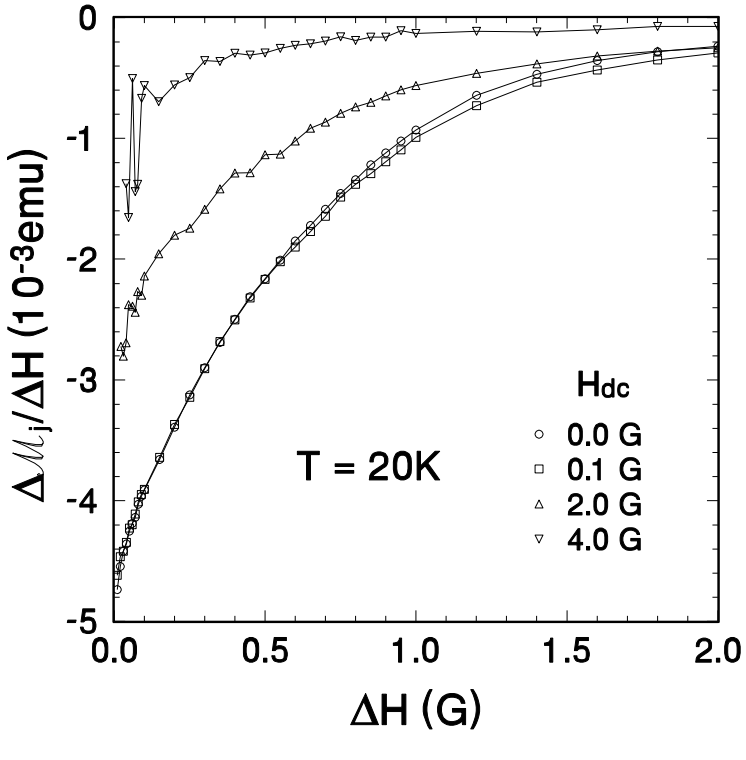
0
-1
-2
-3
-4
-5
0.0
0.5
1.0
1.5
2.0
ΔH (G)
Δ𝓜j/ΔH (10-3emu)
T = 20K
Hdc
0.0 G
0.1 G
2.0 G
4.0 G

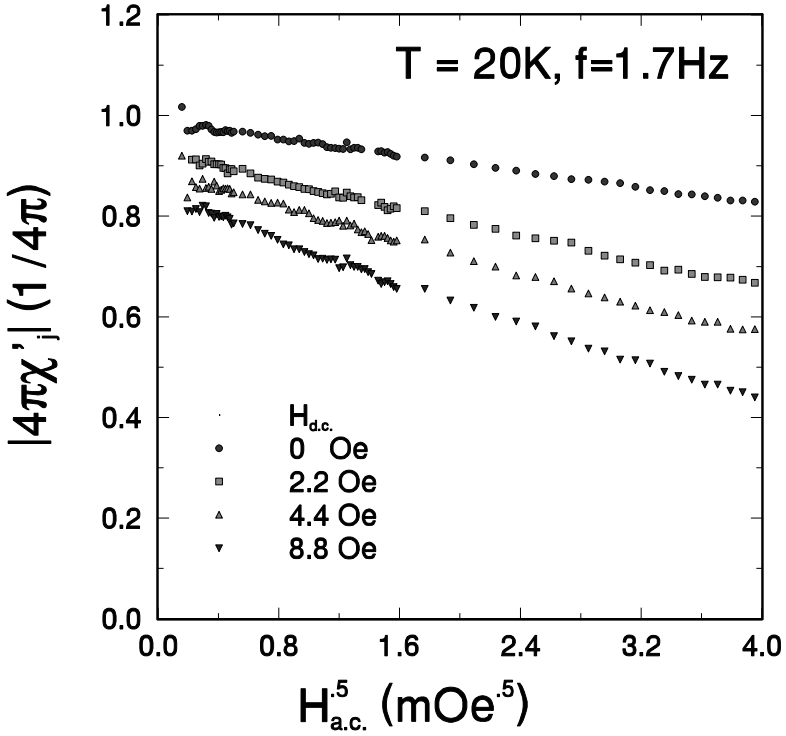
T = 20K, f=1.7Hz
$|4\pi\chi'_j|$ (1 /4π)
$H^{.5}_{a.c.}$ (mOe$^{.5}$)
1.2
1.0
0.8
0.6
0.4
0.2
0.0
0.0
0.8
1.6
2.4
3.2
4.0
$H_{d.c.}$
0 Oe
2.2 Oe
4.4 Oe
8.8 Oe

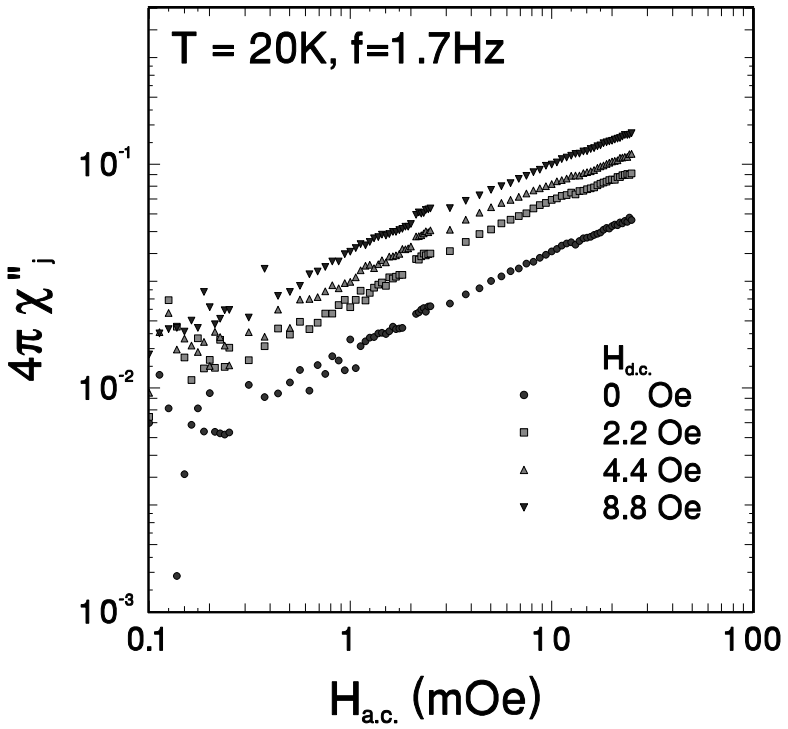
T = 20K, f=1.7Hz
$4\pi\chi''_j$
10^{-1}
10^{-2}
10^{-3}
0.1
1
10
100
$H_{a.c.}$ (mOe)
$H_{d.c.}$
0 Oe
2.2 Oe
4.4 Oe
8.8 Oe